JOURNAL OF NEUROTRAUMA 34:1209–1226 (March 15, 2017)

DOI: 10.1089/neu.2016.4498

Characterization of the Antibody Response after Cervical Spinal Cord Injury

Antigona Ulndreaj,[1,2] Apostolia Tzekou,[1] Andrea J. Mothe,[1] Ahad M. Siddiqui,[1] Rachel Dragas,[1,2] Charles H. Tator,[1–4] Emina E. Torlakovic,[5] and Michael G. Fehlings[1–4]

Abstract

The immune system plays a critical and complex role in the pathobiology of spinal cord injury (SCI), exerting both beneficial and detrimental effects. Increasing evidence suggests that there are injury level–dependent differences in the immune response to SCI. Patients with traumatic SCI have elevated levels of circulating autoantibodies against components of the central nervous system, but the role of these antibodies in SCI outcomes remains unknown. In rodent models of mid-thoracic SCI, antibody-mediated autoimmunity appears to be detrimental to recovery. However, whether autoantibodies against the spinal cord are generated following cervical SCI (cSCI), the most common level of injury in humans, remains undetermined. To address this knowledge gap, we investigated the antibody responses following cSCI in a rat model of injury. We found increased immunoglobulin G (IgG) and IgM antibodies in the spinal cord in the subacute phase of injury (2 weeks), but not in more chronic phases (10 and 20 weeks). At 2 weeks post-cSCI, antibodies were detected at the injury epicenter and co-localized with the astroglial scar and neurons of the ventral horn. These increased levels of antibodies corresponded with enhanced activation of immune responses in the spleen. Higher counts of antibody-secreting cells were observed in the spleen of injured rats. Further, increased levels of secreted IgG antibodies and enhanced proliferation of T-cells in splenocyte cultures from injured rats were found. These findings suggest the potential development of autoantibody responses following cSCI in the rat. The impact of the post-traumatic antibody responses on functional outcomes of cSCI is a critical topic that requires further investigation.

Keywords: antibody-secreting cells (ASCs); astrocytes; autoantibodies; cervical spinal cord injury (cSCI); IgG/IgM immunoglobulins

Introduction

Mounting evidence indicates that the pathobiology of spinal cord injury (SCI) is in part determined by the injury level; thus, it seems intuitive that therapeutic interventions should be designed to take into account level-specific mechanisms.[1] Despite advances in medical, surgical, and rehabilitation approaches, there is a major need for effective neuroprotective or neuroregenerative treatment options to enhance functional recovery following SCI. In the U.S. alone, more than 1 million individuals are estimated to suffer from the effects of SCI, the majority of whom are affected at the cervical level.[2,3] With the increased incidence of SCI due to falls in the elderly, the number of injured persons awaiting treatment is anticipated to rise.[4]

The immune system plays a pivotal role following SCI and the key pathways could be harnessed for the development of effective treatments.[5] Although cervical SCI (cSCI) is the predominant level of injury seen clinically, research on the important immune-related mechanisms underlying the pathophysiology of SCI at this level has been limited. Delineating these mechanisms in cSCI is crucial for the creation of clinically relevant immune-based interventions.[6]

Recent evidence has suggested that autoantibodies—immunoglobulins acting against components of the spinal cord—may be important factors in the pathophysiology of SCI. Higher levels of serum autoantibodies against myelin basic protein (MBP) and GM-1 gangliosides are observed in patients with SCI.[7,8] Moreover, SCI patients exhibit increased expression of the B-cell activating factor of the tumor necrosis factor family, a proliferation-inducing ligand and B-cell maturation antigen in peripheral blood mononuclear cells, which are associated with autoantibody-mediated pathologies.[9] Despite the evidence for the existence of autoantibodies in spinal cord–injured patients, their role in recovery after SCI in humans is unknown. Of note, mice lacking B-cells were shown to have improved outcomes following

[1]Division of Genetics and Development, Toronto Western Research Institute and University of Toronto Spinal Program, Krembil Neuroscience Center, University Health Network, Toronto, Ontario, Canada.
[2]Institute of Medical Science, Faculty of Medicine, [3]Department of Surgery, [4]University of Toronto Spine Program, [5]Department of Laboratory Hematology, University of Toronto, Toronto, Ontario, Canada.

mid-thoracic SCI, suggesting that autoantibodies are pathogenic.[10,11] In addition, the effects of antibody-mediated autoimmunity after SCI may be systemic, as SCI induces autoantibodies not only against the spinal cord, but also against systemic antigens.[12]

However, as humoral immunity is dysregulated in an injury level–dependent fashion following SCI,[13–15] it is important to know whether changes in humoral immunity after cSCI impact the development of autoantibodies. In this study we investigated the antibody response after cSCI by addressing three main aims: 1) to determine the duration of antibody deposition in the spinal cord during the subacute and chronic phases, compared with sham; 2) to identify prominent cell types targeted by antibodies in the lesioned spinal cord; and 3) to characterize the peripheral antibody immune responses in the spleen, which is one of the organs responsible for the generation of immunoglobulins. Our results demonstrate significant accumulation of antibodies in the injured spinal cord and their co-localization with astrocytes and neurons. These phenomena, which were seen in parallel with enhanced antibody responses in the spleen, were limited in the subacute phase of injury.

Methods

Animals and surgical procedure

A total of 141 adult female Wistar rats were used for this study (Charles River; 8 weeks old, 250–300 g). All protocols for animal handling and treatments were applied in accordance with the standards of the Animal Use Committee of the University Health Network. All surgical procedures were performed under anesthesia using 2% isoflurane delivered in a 1:1 mixture of oxygen and nitrous oxide. Sham animals underwent C7-T1 laminectomy, leaving the exposed spinal cord intact. The injured group received a clip compression injury for 60 sec using a 35 g modified aneurysm clip, which was applied extradurally at the C7-T1 level, as previously established (Fig. 1A).[16] Muscles were sutured and the skin was closed with Michel wound clips. All animals were given a subcutaneous injection of 1 mL buprenorphine (0.05 mg/kg) and 5 mL saline immediately post-surgery and twice a day for 2 days after surgery. After the injury or laminectomy, the animals were kept in the animal facility of the Krembil Research Institute where food and water were provided *ab libitum.* Manual bladder expression

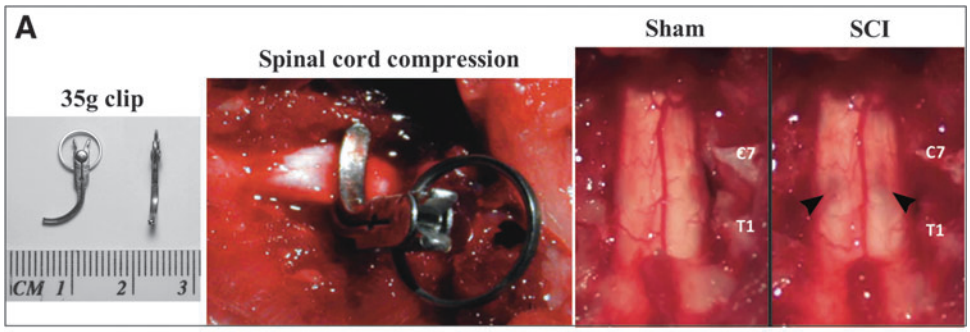

B

Assessment	2 weeks post SCI (Subacute phase)	10 weeks post SCI (Early chronic phase)	20 weeks post SCI (Late chronic phase)
Quantification of IgG and IgM Abs in spinal cord protein extract (WB)	✔	✔	✔
Detection of IgG and IgM Abs in spinal cord sections (IF)	✔		
Quantification of IgG and IgM Abs in CSF (ELISA)	✔		
Identification of astrocytes as a cell target of autoantibodies in the spinal cord (IHC)	✔		
Binding of sérum Abs to fixed astrocytes *in vitro* (IF)	✔		
Counts of splenic IgG and IgM plasma cells (IHC)	✔	✔	✔
Secretion of IgG and IgM Ab *in vitro* (ELISA)	✔	✔	✔
T-cell proliferation *in vitro* (flow cytometry)	✔	✔	✔
Quantification of total and autoreactive Abs in serum (ELISA)	✔		

FIG. 1. Summary of experimental approach. **(A)** Clip compression injury model at the C7-T1 level. From left to right representative images of: 1) a modified aneurism clip used to impact the spinal cord; 2) clip compression injury of the spinal cord; 3) a spinal cord after laminectomy (Sham) and after clip compression (SCI). Note the bruising of the spinal cord created immediately after clip injury. **(B)** Table summarizing the time-points post-SCI studied and the experimental approaches taken for the characterization of the antibody responses after cervical SCI. SCI, spinal cord injury; WB, Western blot; IF, immunofluorescence; CSF, cerebrospinal fluid; ELISA, enzyme-linked immunosorbent assay; IHC, immunohistochemistry. Pictures of panel (A) are courtesy of Dr. Rakhi Sharma and Jared Wilcox. Color image is available online at www.liebertpub.com/neu

was performed three times a day. Animals that showed signs of infection were excluded from the study. Animals were sacrificed at 2 (subacute phase), 10 (early chronic phase), and 20 (later chronic phase) weeks post-injury.[17]

Animal sacrifice and tissue collection

At the experimental end-points of the study, animals were deeply anesthetized using isoflurane, and blood was collected by cardiac puncture prior to transcardial perfusion. The animals were perfused with either phosphate-buffered saline (PBS) alone, or PBS followed by 4% paraformaldehyde (PFA) in PBS, in order to collect fresh or fixed tissues, respectively. Prior to sacrifice, animal body weights were recorded. Figure 1B provides an overview of the experiments conducted and the time-points assessed in the present study.

Western blot semi-quantification of IgG and IgM immunoglobulins in the spinal cord

Levels of immunoglobulin G (IgG) and IgM immunoglobulins in spinal cord protein lysates were assessed at 2, 10, and 20 weeks post-SCI by Western blotting. Five (5) mm long spinal cord segments centered at the injury epicenter were isolated from PBS only–perfused animals, snap frozen, and stored in −80°C until all samples were collected for the study. Then, spinal cords were crushed manually and further homogenized in radioimmunoprecipitation assay (RIPA) buffer supplemented with protease inhibitors, according to the manufacturer's instructions (Thermo Scientific), using a small motorized homogenizer. Total protein concentration of the clear supernatant was determined by bicinchoninic acid (BCA) assay, based on a bovine serum albumin (BSA) standard curve, according to the manufacturer's instructions (Thermo Scientific). Samples were aliquoted for each experiment to avoid repetitive freeze-thawing and stored at −80°C. Protein extracts (10 μg/sample, four samples/group), purified rat IgG (0.05 μg; Sigma) and purified rat IgM (0.02 μg; Invitrogen) were resolved in a 10% sodium dodecyl sulfate (SDS)-acrylamide gel and subsequently transferred to a polyvinylidene fluoride membrane for 2 h at 100 V without SDS. Membranes were blocked for 1 h at room temperature with 5% nonfat milk in 0.1% Tween 20-Tris-buffered saline (TBS). Next, the membranes were blotted with horseradish peroxidase (HRP)-conjugated anti-rat IgG (1:10,000; Thermo Scientific) or anti-rat IgM (1:5000; Thermo Scientific) antibodies for 2 h at room temperature. Membranes were exposed to film, then washed and re-blotted with anti-mouse glyceraldehyde-3-phosphate dehydrogenase (GAPDH) antibody (1:20,000; Abcam) for 30 min at room temperature and next with goat anti-mouse HRP antibody (1:20,000; Sigma) for another 30 min at room temperature, followed by another exposure to film. ImageJ software (National Institutes of Health) was used to quantify the protein bands using the appropriate plugin.

Assessment of endogenous antibody deposition in the spinal cord at 2 weeks post-cSCI by immunofluorescence microscopy

Spinal cords from rats perfused with 4% PFA were post-fixed overnight in 10% sucrose (in 4% PFA-PBS) and cryo-protected in 20% sucrose in PBS, also overnight. A 2-cm long segment of spinal cord centered at the injury epicenter was embedded in OCT Tek embedding matrix in dry ice and transverse sections of 30 μm were taken on glass slides and stored at −80°C until used for staining. Sections were dried at room temperature (20 min), rehydrated once with PBS (10 min) and subsequently blocked with 5% donkey serum (DS) + 1% BSA + 0.3% Triton X-100 in PBS for 1 h at room temperature. Primary goat anti-rat IgM antibody (1:100, Invitrogen) was incubated overnight at 4°C, followed by fluorescent-tagged secondary antibody (Alexa Fluor 488, 1:200; Life Technologies) and 4′,6-diamidino-2-phenylindole (DAPI; 1:400), also overnight at 4°C. Next, sections were blocked with 5% goat serum (GS) + 1% BSA + 0.3% Triton X-100 in PBS for 1 h and stained with fluorescent-conjugated anti-rat IgG antibody (Alexa Fluor 568, 1:150; Life Technologies) for 2 h at room temperature. Sections were washed four times with PBS between staining steps. Slides were cover-slipped with Mowiol mounting medium (Sigma). To avoid staining variability, all samples were stained at the same time.

Samples were selected randomly for imaging and images were acquired as close together as possible. For this assessment, a Nikon Eclipse E800 epifluorescence microscope at 10× magnification was used. For the detection of IgM deposits, the threshold of the image acquisition equipment was set up such that the signal from the control staining (secondary antibody alone) was zero; for IgG (for which a directly fluorescent-tagged antibody was used), the threshold was set such that the brightest sections (injury epicenter) were not overexposed yet signal from the least bright sections could still be detected. As a result, we determined 2000 msec to be the optimum exposure time for imaging of IgG and IgM—a time short enough to avoid over-saturation and over-quenching of the samples. All settings were kept constant during imaging. The intensity of the detected fluorescence, excluding the signal from the dura, was measured with the appropriate plugin in ImageJ software and assessed under identical conditions. As a positive control for IgG and IgM immunoglobulin staining, 30-μm thick rat spleen sections were stained using the same protocol as for the spinal cord.

Competition assay

To exclude the possibility of non-specific IgM staining in injured spinal cord sections, we stained adjacent sections with the secondary fluorescent-tagged antibody only. Because we used a directly conjugated anti-rat IgG antibody for the detection of rat IgG in the spinal cord, we could not perform a secondary-only control experiment. Thus, to confirm specificity of the fluorescent-tagged anti-rat IgG antibody in spinal cord sections, we performed a competition assay with purified polyclonal rat IgG and protein lysate from injured or sham spinal cord at 2 weeks after injury. A random injured spinal cord sample at 2 weeks post-SCI containing the injury epicenter was selected for this assay. Sections were blocked with 5% DS +1% BSA + 0.3% Triton X-100 in PBS for 1 h at room temperature. Nuclear staining with DAPI (1:400) was done overnight at 4°C, after which sections were washed four times with PBS. Sections were then blocked with 5% GS +1% BSA + 0.3% Triton X-100 for 1 h at room temperature.

For the competition assay, the anti-rat IgG detection antibody (Alexa Fluor 568, 1:150; Life Technologies) was pre-incubated with 53.3 times molar excess of either purified rat IgG (Sigma) or spinal cord protein lysate prior to staining the spinal cord sections. The pre-incubation was done for 1 h at room temperature using low-binding tubes to minimize binding of antibodies on the tube. The 53.3 times molar ratio excess was selected because this was the highest possible concentration we could use, given the total protein concentration of our spinal cord protein samples. To calculate the molarity of the spinal cord protein lysate, we used 50 kDa as the protein's average molecular weight. This was determined by multiplying the average length of eukaryotic proteins (449 ± 25 amino acids)[18] by the average amino acid weight (110 Da). Binding of the fluorescent anti-rat IgG-detecting antibody to the spinal cord sections was done at room temperature for 2 h, after which the slides were washed, mounted, and cover-slipped. Images were taken with a Leica epifluorescence microscope at 10× magnification and fluorescence intensity was determined with ImageJ, as described above.

Immunofluorescence staining for GFAP, CSPG, NF200, IgG, and IgM in the spinal cord at 2 weeks post-cSCI

To detect binding of endogenous immunoglobulins to astrocytes and neurons at 2 weeks post-cSCI, we stained spinal cord sections for rat glial fibrillary acidic protein (GFAP), chondroitin sulfate

proteoglycans (CSPG), or neurofilament-200 (NF200), and co-labeled for rat IgG and IgM.

For co-labeling with IgG + GFAP, sections were blocked with 5% DS +1% BSA +0.3% Triton X-100 in PBS for 1 h at room temperature, and incubated with anti-GFAP antibody (1:500; Millipore), overnight at 4°C. After washing, sections were blocked with 5% GS +1% BSA +0.3% Triton X-100 for 1 h at room temperature and incubated with fluorescent-tagged secondary antibody (Alexa Fluor 488, 1:200; Life Technologies) and DAPI (1:400) overnight at 4°C. Lastly, fluorescent-tagged anti-rat IgG antibody (Alexa Fluor 568, 1:150; Life Technologies) was applied for 2 h at room temperature.

For co-labeling with IgM + GFAP, sections were blocked with 5% DS +1% BSA +0.3% Triton X-100 in PBS for 1 h at room temperature, and incubated with anti-rat IgM (1:100; Invitrogen) overnight at 4°C, followed by fluorescent-tagged secondary antibody (Alexa Fluor 488, 1:200; Life Technologies) and DAPI (1:400), also overnight at 4°C. Next, sections were incubated with anti-GFAP antibody (1:500; Millipore) overnight at 4°C, re-blocked with 5% GS +1% BSA + 0.3% Triton X-100 for 1 h at room temperature, and incubated with fluorescent-tagged secondary antibody (Alexa Fluor 568, 1:200; Life Technologies), washed, and cover-slipped.

For co-labeling with IgG + IgM + GFAP or IgG + IgM + CSPG, sections were blocked with 5% DS +1% BSA + 0.3% Triton X-100 in PBS and incubated with anti-rat IgM (1:100, Invitrogen) overnight at 4°C, followed by fluorescent-tagged secondary antibody (Alexa Fluor 488, 1:200; Life Technologies) as described above. Then, anti-GFAP or anti-CSPG antibody (mouse anti-CSPG, 1:200; Sigma) was applied overnight, followed by re-blocking with 5% GS + 1% BSA +0.3% Triton X-100 in PBS for 1 h at room temperature. Secondary antibody (Alexa Fluor 647, 1:200; Life Technologies) and DAPI (1:400) were applied overnight at 4°C. Lastly, fluorescent anti-rat IgG antibody was incubated for 2 h at room temperature as described above, and sections were cover-slipped and stored in −20°C until imaged.

For co-labeling with IgG + NF200, sections were blocked with 5% DS +1% BSA +0.3% Triton X-100 in PBS and incubated with anti-rat NF200 antibody (1:200; Sigma) overnight at 4°C. After washing, tissue sections were blocked with 5% GS + 1% BSA +0.3% Triton X-100 for 1 h at room temperature and incubated with fluorescent-tagged secondary antibody (Alexa Fluor 488, 1:200; Life Technologies) and DAPI (1:400) overnight at 4°C. Lastly, fluorescent-tagged anti-rat IgG antibody (Alexa Fluor 568, 1:150; Life Technologies) was applied for 2 h at room temperature.

For co-labeling with IgG + CD45RA + GFAP, spinal cord sections containing the injury epicenter were blocked with 5% DS +1% BSA +0.3% Triton X-100 in PBS and incubated overnight at 4°C with anti-rat CD45RA (1:200; BD Biosciences), blocked with 5% GS + 1% BSA +0.3% Triton X-100 in PBS and incubated with secondary antibody (Alexa Fluor 488, 1:400; Life Technologies) for 2 h at room temperature. Following washes, sections were incubated with anti-GFAP primary antibody (1:500; Millipore) overnight at 4°C followed by a re-blocking step with 5% GS +1% BSA +0.3% Triton X-100 in PBS and incubation with a secondary antibody overnight at 4°C as mentioned above. Last, anti-rat IgG antibody and DAPI were added for 2 h at room temperature. Spleen sections were used as a positive control for the IgG + CD45RA staining.

Imaging settings were set based on sections where the primary antibody for IgM, NF200, GFAP, or CSPG was omitted, such that the signal from the secondary-only stained sections was zero. Low-power images (10×) were taken with a Nikon Eclipse E800 epi-fluorescence microscope, whereas high-power confocal images were taken with a LSM 510 Meta microscope.

Assessment of binding of serum IgG and IgM antibodies to fixed astrocytes in vitro

To confirm that binding of immunoglobulins to astrocytes in the lesioned spinal cord is specific rather than a result of sequestration,[19] rat astrocytes were fixed in culture and incubated with serum from rats with cSCI or laminectomy only (sham) at 2 weeks post-injury, and binding of IgG and IgM was determined microscopically. Rat primary cortical astrocytes (Gibco) were cultured in Dulbecco's modified Eagle's medium F12 (DMEM-F12; Gibco) containing 100 U/mL penicillin, 100 μg/mL streptomycin (Gibco) and 10% fetal bovine serum (FBS) in 10 cm^2 dishes at 37°C and 5% CO_2 until they were 80% confluent. The cells were then split and seeded at 25,000 cells/well in a 24-well plate on top of 12 mm glass cover-slips. The astrocytes were then grown in serum-free DMEM for 5 days, fixed with 4% PFA in PBS for 10 min at room temperature, and washed twice with PBS. Fixed astrocytes were blocked with 5% DS +1% BSA + 0.3% Triton X-100 in PBS for 1 h at room temperature. Next, 10% of rat serum from animals with cSCI or sham injury was incubated in duplicate with astrocytes for 2 h at room temperature. The same protocol described above for IgG + IgM + GFAP staining was applied. Images from three random fields were taken at 20× magnification, and intensity of detected fluorescence was quantified with ImageJ. The obtained values were averaged for each serum sample and then averaged between the samples of the same group ($n = 5$/group).

Immunohistochemical detection of splenic IgG+ and IgM+ ASCs

Frequencies of splenic antibody secreting cells (ASCs) increase with age.[20] Thus, to determine changes of IgG and IgM ASCs in the spleen in the course of 20 weeks, we included age-matched control groups (naïve) for all time-points of this assessment.

Four (4) μm thick formalin-fixed, paraffin-embedded sections were de-waxed in five changes of xylene and treated with a graded series of alcohols. Heat-induced epitope retrieval (HIER) method with Tris-ethylenediaminetetraacetic acid (EDTA) buffer at pH 9.0 was applied. Endogenous peroxidase and biotin activities were blocked using 3% hydrogen peroxide and avidin/biotin blocking kit (Vector Laboratories), respectively. For detection of IgM+ ASCs, sections were blocked for 10 min with 10% normal GS. Subsequently, they were incubated with the primary antibody (1:500; Rockland) for 1 h at room temperature. This was followed by a biotin-labeled secondary antibody (Vector Laboratories) for 30 min and HRP-conjugated ultra-streptavidin labeling reagent (ID Labs. Inc., Canada) for 30 min. After washing well in TBS, color development was completed with freshly prepared 3,3'-diaminobenzidine (DAB) solution (Dako). For detection of IgG+ ASCs, sections were blocked as above, then incubated with HRP-conjugated anti-rat IgG antibody (1:50; Thermo Scientific) overnight at 4°C, and followed by color development using freshly prepared DAB solution. Finally, IgG and IgM stained sections were counterstained lightly with Mayer's Hematoxylin, dehydrated in alcohols, cleared in xylene and mounted in Permount mounting medium (Fisher).

To quantify the number of IgG+ and IgM+ ASCs, we counted IgG+ or IgM+ positive cells with typical ASC characteristics (small, round cells with very intense IgG or IgM cytoplasmic staining) in 10 randomly selected consecutive fields (0.785 mm^2). Technically suboptimal fields were skipped. All positive cells in each appropriate field were counted. These assessments were conducted by an experienced pathologist (author E.E.T.) who was blinded to the groups of the study.

Detection of immunoglobulins in CSF

To examine whether parenchymal immunoglobulins derive from intrathecal synthesis, we measured levels of immunoglobulins in cerebrospinal fluid (CSF) of rats with SCI or sham injury at 2 weeks by enzyme-linked immunosorbent assay (ELISA). Aliquots of 50 μL CSF were collected through lumbar puncture at the L3-L4 level as previously described.[21] ELISA kits (Abcam) were used for the quantification of IgG and IgM immunoglobulins following

manufacturer's instructions. Prism (Graph Pad) was used to interpolate the unknown concentrations from the standard curves.

Flow cytometric analysis of the frequency of splenic T- and B-lymphocytes

Immediately after PBS perfusion, spleens ($n = 6$/group) were dissected, transferred in 2% FBS in PBS and mechanically dissociated through a 70-μm nylon mesh strainer. Red blood cells were lysed (0.1 mM EDTA, 10 mM $KHCO_3$, 150 mM NH_4Cl) for 5 min at room temperature, and samples were centrifuged at 2000 rpm for 5 min. The pelleted cells were washed with 2% FBS in PBS. The number of viable cells was quantified with trypan blue and 106 viable cells/ tube were incubated with the FcγR blocker (Innovex) for 20 min on ice. Next, the samples were stained with fixable viability dye eFluor 780 (1:1000; Life Technologies) for 20 min at 4°C and subsequently with CD45-FITC (leukocytes; BD Biosciences), CD3-PE (T- lymphocytes; BD Biosciences) and CD45RA-V450 (B-lymphocytes; BD Biosciences). An LSR II flow cytometer was used for data acquisition, where at least 10,000 events of viable cells were collected. FlowJo V10 (Trestar) was used for data analysis and gating of positive populations was performed based on appropriate isotype-matched antibody controls (all from BD Biosciences).

Preparation of injured spinal cord homogenates for in vitro stimulation of splenocytes

Five (5) mm long spinal cord segments centered at the injury epicenter were aseptically isolated from PBS-only perfused animals, snap frozen, and stored in −80°C until all spinal cord samples were collected for this assay. Spinal cords were fully thawed at room temperature and snap frozen again to allow for one freeze-thaw cycle and to facilitate cell lysis. Subsequently, samples were crushed manually and further homogenized in ddH_2O without protease inhibitors by using a Dounce homogenizer (VWR International). The samples were spun down at 12,200 rpm for 20 min at 4°C. All the above steps were performed under aseptic conditions and great effort was made to process samples on ice in order to maintain protein integrity, given that a protease inhibitor was not used. The clear supernatant was collected and its total protein concentration was determined by BCA assay, based on a BSA standard curve, according to the manufacturer's instructions (Thermo Scientific). Samples were aliquoted for each experiment to avoid repetitive freeze-thawing and stored at −80°C until used.

With this protocol, we aimed for the total protein extraction with H_2O to be as successful as the extraction with RIPA. To determine this, we extracted proteins from the spinal cord using the established RIPA (+inhibitors) extraction protocol as described above. Next, 40 μg of total spinal cord protein (extracted with H_2O or RIPA) were run in a 12% SDS-acrylamide gel under reducing conditions. The gel was then stained with Coomasie blue and similarity of stained bands between the two extraction methods was visually determined (data not shown). Thus, the H_2O method was selected over RIPA to avoid any effects that RIPA (+inhibitors) may have for the *in vitro* stimulation protocol.

Detection of immunoglobulins secreted by stimulated splenocytes in vitro

Spleens ($n = 4$/group) from PBS-perfused rats were harvested under aseptic conditions and transferred in complete RPMI medium (10% heat inactivated FBS, 55 mM β-mercaptoethanol, 1M HEPES, 200 mM L-glutamine, and 100 U/mL penicillin-streptomycin solution in RPMI 1640 medium). Single cell suspensions were prepared by mechanical dissociation through a 70-μm nylon mesh cell strainer and red blood cells were lysed as described above. Next, 250,000 cells/well were allocated in a sterile round bottom 96-well plate and stimulated *in vitro*. Pooled protein extract ($n = 3$/group) from the spinal cord of injured rats at 2, 10, and 20 weeks post-cSCI, respectively, was added (100 μg/mL) into cultures of sham- or SCI-derived splenocytes from the matching time-point. All conditions were performed in duplicate. For each sample, two wells that did not receive any stimulation served as negative controls. After 3 days in culture, supernatants were collected and stored at −80°C.

To determine levels of secreted IgG and IgM immunoglobulins by stimulated splenocytes *in vitro,* a sandwich ELISA was developed in-house. ELISA plates were coated with 2 μg/mL of rabbit anti-rat IgG or goat anti-rat IgM antibody (both from Abcam) overnight at 4°C. Plates were washed once with PBS and blocked with 4% GS in PBS for 2 h at room temperature. Culture supernatants were diluted 1:10 and 1:5 for detection of IgG and IgM immunoglobulins, respectively. These dilutions were chosen because detection values of all samples fell within the linear range of the standard curve. For the standard curve, polyclonal rat IgG (Sigma) and monoclonal rat IgM (Invitrogen) antibodies of known concentrations were used in serial dilutions, covering the range of 1 μg/mL-0.03 ng/mL. Samples and standards were run in duplicate. The supernatants and the purified immunoglobulins were incubated for 4 h at room temperature. Following washes with 0.05% Tween 20-PBS, HRP-tagged anti-rat IgG or anti-rat IgM detecting antibody (1:1000; Thermo Scientific) was added for 30 min at room temperature. Plates were washed and developed with ultra-fast TMB substrate solution (Thermo Scientific) and neutralized with 2 M Sulfuric Acid (Sigma). Lastly, absorbance at 450 nm was measured with an ELISA plate reader. The concentrations of IgG and IgM in samples were interpolated from the standard curve to which a 4PL nonlinear curve fit was applied using the Prism (Graph Pad) software. For each sample, the concentration of immunoglobulins under stimulation was normalized to the concentration of immunoglobulins detected in cultures under no stimulation. SPSS Statistics (IBM) was used for statistical analysis.

Assessment of splenic T-cell activation against injured spinal cord homogenate in vitro

Splenic activation against homogenate from the injured spinal cord was assessed based on T-cell proliferation. Fresh spleens ($n = 4$/group) were harvested under aseptic conditions and transferred in complete RPMI medium (10% heat inactivated FBS, 55 mM β-mercaptoethanol, 1 M HEPES, 200 mM L-glutamine, and 100 U/mL penicillin-streptomycin solution in RPMI 1640 medium). Single-cell suspensions were prepared by mechanical dissociation and red blood cells were lysed as described above. Cells were subsequently washed in 1% BSA in PBS and labeled with 10 μM of carboxylfluorescein succinimidyl ester (CFSE) according to the manufacturer's instructions (eBioscience). Next, 250,000 cells/well were allocated into a sterile round bottom 96-well plate and stimulated *in vitro:* Homogenate (100 μg/mL)—pooled from the spinal cord of injured rats ($n = 3$/group) at 2, 10, and 20 weeks post-cSCI—was added to cultures of sham- or SCI- derived splenocytes from the matching time-point. As a positive control for T-cell proliferation, samples were stimulated with the potent T-cell mitogen concanavalin A (ConA) (1μg/mL, Sigma). For each sample, a negative control was prepared where no antigen was added to the culture. All conditions were performed in duplicate. Cells were cultured at 37°C for 3 days. Next, they were washed in flow cytometry buffer (2% FBS in PBS) and incubated with FcγR blocker (Innovex) for 20 min on ice. The samples were then stained for 20 min at 4°C with fixable viability dye eFluor 780 (1:1000; Life Technologies) according to the manufacturer's instructions and subsequently with CD3-PE (T- lymphocytes; BD Biosciences) for 30 min at 4°C. An LSR II flow cytometer was used for data acquisition, where at least 10,000 events of viable cells were collected. T-cell proliferation was assessed with the FlowJo V7 plugin

for cell proliferation. Division index, which refers to the number of divisions each cell in the culture has undergone, was the parameter used to evaluate T-cell proliferation (www.flowjo.com/v6/html/proliferation.html). For this analysis, the signal from matched non-stimulated samples was used as a baseline.

Detection of spleen germinal centers

Four (4) μm thick formalin-fixed, paraffin-embedded sections were de-waxed in five changes of xylene and treated with a graded series of alcohols. HIER method with Tris-EDTA buffer at pH 9.0 was applied. Endogenous peroxidase was blocked using 3% hydrogen peroxide. Rabbit anti- B-cell lymphoma 6 (Bcl-6) antibody (1:1000; Santa Cruz) was applied overnight at 4°C. An anti-rabbit IgG ImmPRESS polymer system (Vector Laboratories) was used for detection, following manufacturer's instructions. Color development was completed with freshly prepared DAB solution (Dako). Last, sections were counterstained lightly with Mayer's Hematoxylin, dehydrated in alcohols, cleared in xylene and mounted in Permount mounting medium (Fisher).

Quantification of serum IgG and IgM antibodies against spinal cord lysate

Blood was collected by cardiac puncture in deeply anaesthetized animals and allowed to clot for 30 min at room temperature. Samples were centrifuged at 2000 rpm for 10 min and serum was collected and stored in −80°C until used for ELISA. ELISA plates were coated overnight at 4°C with 10 μg/mL of pooled ($n = 3$) naïve spinal cord lysate in PBS. Plates were then washed once with PBS and blocked with 1% BSA-PBS for 2 h at room temperature. Serum was diluted at 1:50 and incubated for 4 h at room temperature. Binding of IgG and IgM antibodies was determined by HRP conjugated anti-rat IgG and IgM antibodies and quantification was done based on respective standard curves as described above.

Detection of IgG and IgM antibody levels in serum

To determine total levels of IgG and IgM immunoglobulins, we used our in-house ELISA protocol as described above, with the difference that here serum samples were diluted 1: 50,000 and 1:1,000,000 for the detection of IgM and IgG immunoglobulins, respectively. Each sample was assessed in duplicate. Concentration of IgG and IgM was determined based on the respective standard curves as described.

Statistical analysis

SPSS Statistics (IBM) was used for statistical analysis of all results. Data that met the criteria for parametric statistical analysis were subjected to means tests (independent *t*-test for two groups or analysis of variance [ANOVA] for more than two groups of samples, with Bonferroni *post hoc* test where appropriate). Non-parametric statistical analysis was performed for non-parametric data (Mann-Whitney for two groups and Kruskal Wallis for more than two groups). Where necessary, variance-stabilizing transformations were used to meet the requirements for parametric statistical analysis. The significance level of all analyses was set to $p < 0.05$. Data are presented as mean ± standard error of the mean (SEM).

Results

Higher levels of IgG and IgM immunoglobulins are detected in the lesioned spinal cord at 2 weeks post-cSCI

At 2 weeks, rats with cSCI had significantly higher levels of IgG and IgM immunoglobulins in their spinal cord than in sham rats, as revealed by Western blot (Fig. 2A, 2B). Immunoglobulin levels at 10 and 20 weeks post-SCI were not significantly different between groups (Fig. 2A, 2B). At 2 weeks post-cSCI, immunofluorescence (IF) staining against rat IgG and IgM antibodies in spinal cord sections spanning a distance of 1.5 cm centered at the injury epicenter, demonstrated increased binding of IgG and IgM in the lesioned spinal cord (Fig. 2C, 2D). In addition to confirming the Western blot data, the IF approach provided evidence for the distribution of immunoglobulins relative to the injury epicenter, showing that immunoglobulins accumulated around the injury epicenter and declined with increasing distance from it (Fig. 2D).

The detected signal for binding of immunoglobulins to the lesioned spinal cord was specific, as the secondary-only control for IgM staining resulted in negligible binding (data not shown) and the competition assay for the directly conjugated fluorescent anti-rat IgG detecting antibody confirmed its specificity for rat IgG immunoglobulins. Indeed, purified rat IgG blocked binding of the fluorescent-tagged anti-rat IgG completely (Fig. 2E). Sham-derived and SCI-derived lysates caused partial blocking of the fluorescent antibody (Fig. 2E). However, SCI-derived lysate exhibited a stronger inhibitory effect than the sham-derived lysate, due to higher levels of IgG immunoglobulins in the SCI spinal cords than in shams, as shown by Western blot (Fig. 2A, 2B).

IgG and IgM immunoglobulins bind to astrocytes at 2 weeks post-cSCI

IgM and IgG immunoglobulins were detected in the developing cavity (DC), the astroglial scar surrounding the DC, and in the gray matter (Fig. 3A, 3B). In addition, IgG was present in the posterior white matter and the anterior white matter (Fig. 3B), whereas IgM was detected only in the posterior white matter (Fig. 3B). When we performed double staining for GFAP and IgG, we observed extensive co-localization of IgG immunoglobulins with the GFAP+ glial scar surrounding the DC (Fig. 3C). Similar results were found for IgM and GFAP co-labeling (not shown). As expected, no co-labeling for GFAP and immunoglobulins was observed in the sham group (Fig. 3D). Higher power microscopy images confirmed co-localization of IgG and IgM antibodies with astrocytes surrounding the DC (Fig. 3E), in particular with those expressing CSPG (Fig. 3F). Last, serum IgG and IgM immunoglobulins from rats with cSCI exhibited significantly higher binding to fixed astrocytes *in vitro* than serum from sham rats (Fig. 4).

Endogenous IgG antibodies co-localize with ventral horn neurons

Immunostaining for rat IgG and the neuronal marker NF200 at the injury epicenter showed IgG+ neurons in the ventral horn. IgG co-localized with NF200 mainly within neuronal cell bodies in the gray matter, and no evident co-staining with axonal NF200 in the white or gray matter of the anterior spinal cord was found (Fig. 5).

Detection of IgG+ ASCs in the lesioned spinal cord

In addition to extravasation due to compromised blood–spinal cord barrier (BSCB) following SCI, parenchymal immunoglobulins may originate from the central nervous system (CNS; i.e., from ASCs located within the lesioned spinal cord and/or intrathecal ASCs). IgG+ ASCs, which are IgG-expressing cells with ASC morphology (small, round cells with large and intense fluorescent IgG+ cytoplasm), were detected in the anterior white matter of the lesioned spinal cord at 2 weeks post-injury (Fig. 6A). We detected

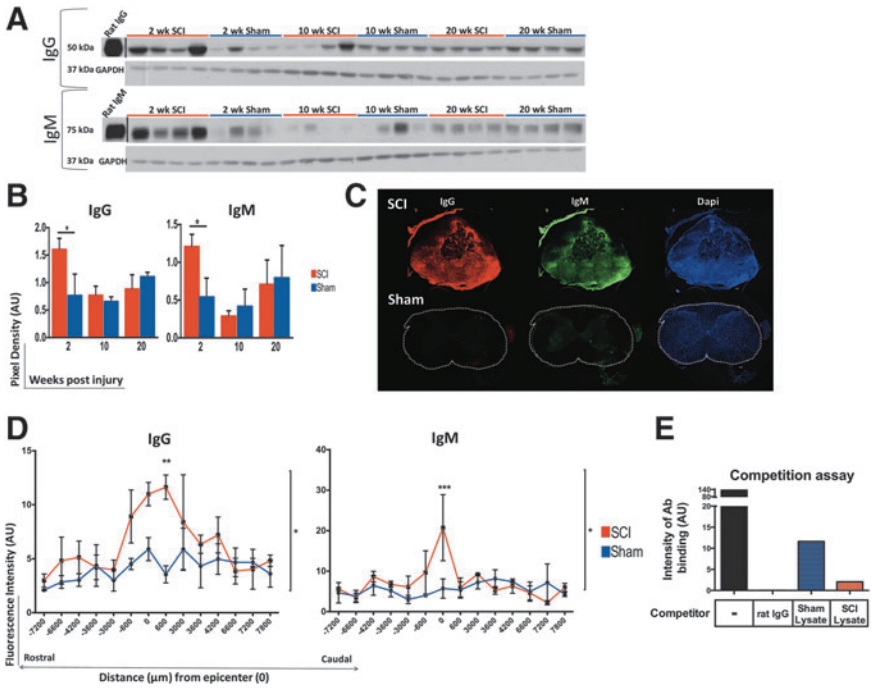

FIG. 2. Increased levels of immunoglobulin G (IgG) and IgM in the lesioned spinal cord at 2 weeks post–cervical spinal cord injury (cSCI). **(A)** Western blot image of IgG and IgM levels in spinal cord protein extract at 2, 10, and 20 weeks in rats with SCI and sham injury. Intensities of the detected signal for the heavy chain of IgG (50 kDa) and IgM (75 kDa), respectively, were normalized to the intensity of the detected housekeeping protein glyceraldehyde-3-phosphate dehydrogenase (GAPDH). **(B)** Semi-quantitative analysis of the detected signal for IgG and IgM antibodies after normalization to GAPDH at 2, 10, and 20 weeks post-injury. Levels of IgG and IgM immunoglobulins increased significantly at 2 weeks post-injury, compared with shams, and returned to levels that were similar to sham controls at 10 and 20 weeks. Independent Student's *t*-test was performed after square normalization of values (this was applied only to IgM data). $*p < 0.05$, $n = 4$/group, mean ± standard error of the mean (SEM). **(C)** Assessment of presence of endogenous IgG and IgM immunoglobulins in the spinal cord with immunofluorescence. Spinal cord sections from injured or sham rats at 2 weeks post-injury, were stained for rat-IgG and IgM. Representative images of spinal cord sections at the injury epicenter of a SCI and a sham sample at a matching level are shown. Images were taken at 10× magnification. Scale bar: 100 μm. **(D)** Quantification of fluorescence intensity of detected IgG and IgM immunoglobulins in serial sections of the spinal cord spanning a total distance of 1.5 cm, centered at the injury epicenter at 2 weeks. Increased deposition of IgG and IgM immunoglobulins peaked at the injury epicenter and was overall statistically higher in the SCI group than in shams. $*p < 0.05$, two-way analysis of variance, Bonferroni *post hoc* test, $n = 3$/group, mean ± SEM. **(E)** Competition assay to determine specificity of the fluorescent tagged anti-rat IgG antibody to spinal cord sections. IgG was pre-incubated either with purified rat IgG, or sham- or SCI-derived spinal cord protein lysate at 53.3 times molar excess of the concentration of the tagged antibody. Purified rat IgG blocked the binding of the fluorescent anti-rat IgG antibody completely. SCI- and sham- derived lysates had a partial blocking effect. Color image is available online at www.liebertpub.com/neu

some IgG+ ASCs also in the dorsal horn of the lesioned spinal cord, as well as inside the DC (not shown). These cells were distinct from astrocytes, as they did not stain for GFAP (Fig. 6B) and as expected, did not stain for the B-cell marker CD45RA. In fact, we did not locate any CD45RA cells in the spinal cord, although our protocol could detect these cells in the spleen (Fig. 6C). We did not find any IgM+ ASCs in the lesioned spinal cord, although we were able to stain IgM+ ASCs in the spleen applying the same protocol (Fig. 6D, 6E). Last, we detected IgG+ ASCs in rat spleens (Fig. 6D, 6F), verifying the specificity of our staining protocol for IgG+ ASCs in the spinal cord. On the other hand, the similar levels of IgG and IgM immunoglobulins in the CSF of both sham and SCI rats at 2 weeks post-injury (Fig. 6G) excluded intrathecal synthesis as a potential source of immunoglobulins in the lesioned parenchyma.

Increased splenic ASC counts at 2 weeks post-cSCI

Rats with cSCI had higher counts of ASCs than sham and naïve rats at 2 weeks (Fig. 7A, 7B), and higher than naïve animals at 10 weeks post-injury (Fig. 7B). Also, sham rats harbored elevated counts of ASCs, compared with naïve rats, at 2 weeks (Fig. 7B). In all time-points of the study, ASC counts were relatively stable in sham animals. However, they increased with age in naïve animals ($p < 0.0001$, one-way ANOVA, Bonferroni *post hoc* test). ASC counts in rats with cSCI decreased with time post-injury ($p < 0.05$, one-way ANOVA, Bonferroni *post hoc* revealed no statistically significant difference between groups). ASC counts leveled off in all groups by the end of our study (Fig. 7B; 20 weeks). These data demonstrate that a) total splenic ASCs increase significantly as a result of cSCI only in the subacute phase, and b) contrary to the naïve group, sham rats are resistant to an age-dependent increase of total ASCs.

Despite the significantly higher ASC numbers at 2 weeks post-cSCI, B-cell frequency in the SCI group was significantly lower than in sham rats (Fig. 7C). B-cell frequency in injured rats recovered to sham levels at 10 and 20 weeks post-injury (Fig. 7C).

When we analyzed changes in splenic ASCs for each class separately (i.e., IgG and IgM), we found that only at 2 weeks post-injury were both IgM+ and IgG+ ASCs higher than in sham rats (Fig. 7D, 7E; 2 weeks). At 10 weeks, IgM ASC counts were higher than shams, whereas IgG ASC counts were lower than shams (Fig. 7D, 7E).

SCI rats maintained increased IgM+ ASCs at all time-points, compared with shams (Fig. 7D), although this was not statistically significant at 20 weeks ($p = 0.218$). IgM+ ASCs were significantly fewer in naïve rats than in the sham or the SCI group at 2 and 10 weeks after injury. All groups had similar IgM+ ASC numbers by the end of the study (Fig. 7D; 20 weeks). Similar to changes in total splenic ASCs (Fig. 7B), IgM+ ASCs increased with age in naïve animals ($p < 0.001$, one-way ANOVA) and remained relatively stable over time in sham rats, whereas in SCI animals a declining trend was observed with time after injury (Fig. 7D).

Despite the initial increase of IgG+ ASCs at 2 weeks post-cSCI, these counts dropped significantly at 10 weeks, compared with shams ($p < 0.05$), and reached similar values at 20 weeks ($p = 0.093$; Fig. 7E). Sham injury caused a statistically significant drop of IgG+ ASC counts, compared with naïve rats, at 2 weeks, but differences between the groups did not persist at subsequent time-points of our study (Fig. 7E). Overall, IgG+ ASC counts increased significantly with age in sham animals but not in the naïve group, as revealed by one-way ANOVA analysis. In the cSCI group, IgG+ ASCs increased significantly from 10 to 20 weeks (one-way ANOVA).

Overall, these data demonstrate that humoral immunity in the spleen is pronounced at 2 weeks due to cSCI, despite the evident decline in total B lymphocytes. However, in the chronic injury phase, IgG immunity declines whereas IgM immunity persists, compared with sham rats.

Increased autoreactive secretion of IgG antibodies by splenocytes in vitro

To determine whether increased splenic ASC counts after cSCI reflect an increased autoreactive humoral response against components of the injured spinal cord, we stimulated sham or SCI-derived splenocytes with injured spinal cord homogenate *in vitro,* and measured the levels of secreted IgG and IgM immunoglobulins by ELISA. In this paradigm, splenocytes from injured rats secreted higher levels of IgG antibodies, compared with shams, at 2 weeks post-injury (Fig. 8). There was no significant difference in the secreted IgM levels between groups at this time-point (Fig. 8). Levels of secreted IgG and IgM immunoglobulin were similar between groups at 10 and 20 weeks after injury (data not shown).

Enhanced autoreactive T-dependent humoral responses at 2 weeks post-cSCI

Increased IgG secretion by splenocytes stimulated with injured spinal cord homogenate *in vitro* suggested that a T-dependent (TD) autoreactive immune response may be favored after cSCI. To test this hypothesis *in vitro,* we stimulated splenocytes with injured spinal cord homogenate and measured proliferation of T-lymphocytes with flow cytometry. Splenocytes from rats with sham injury or cSCI at all time-points of our study (2, 10, and 20 weeks) were incubated with homogenate from injured spinal cord obtained at the matching time-points. T-cell proliferation was measured based on CFSE signal by flow cytometry. Stimulation with T-cell mitogen ConA served as a positive control for T-cell proliferation (Fig. 9A). Splenic T-cells obtained from animals that underwent cSCI displayed significantly higher proliferation capacity, compared with their sham counterparts, when stimulated with homogenate from the injured spinal cord (Fig. 9B; 2 weeks). There was no statistically significant difference in the proliferation response between groups at later time-points (Fig. 9B; 10 and 20 weeks). Upon ConA stimulation, proliferation of splenic T-cells from injured rats was significantly lower at 2 weeks and higher at 10 weeks post-cSCI, compared with shams, whereas there was no difference between groups at 20 weeks (Fig. 9C). Moreover, T-cell frequencies were similar between groups at all time-points studied, as shown with flow cytometry (Fig. 9D, 9E). Last, Bcl6 staining demonstrated the development of germinal centers in the spleens of rats with cSCI (Fig. 9F).

Together, these data show that splenic T-cells have an increased propensity to respond to spinal cord–derived antigens only at 2 weeks after cSCI. This enhanced autoreactivity occurs despite the lower response of T- lymphocytes to ConA stimulation, and is not due to different T-cell numbers in the spleens of injured rats, compared with sham animals. Detection of germinal centers further confirms the maturation of TD responses in SCI animals.

Similar levels of serum autoantibodies to spinal cord protein lysate but depressed levels of total immunoglobulins following cSCI

It was previously shown that transfer of serum immunoglobulins from mice with SCI to naïve mice causes inflammation and paralysis.[10] Here, we measured binding of IgG and IgM immunoglobulins derived from rats with cSCI or sham injury at 2 weeks to naïve spinal cord lysate with ELISA. We found no significant difference in IgG and IgM binding between groups, although four of seven (4/7) rats with cSCI had IgG autoantibodies, compared with two of seven (2/7) in the control group (Fig. 10A). However, levels of total serum IgG and IgM immunoglobulins were significantly depressed in rats with cSCI, compared with shams (Fig. 10B).

FIG. 3. Binding of endogenous immunoglobulins to astrocytes of the lesioned spinal cord. **(A)** Hematoxylin/eosin (HE) and luxol fast blue (LFB) stained section showing the injury epicenter at 2 weeks post–cervical spinal cord injury (cSCI). Black inset shows the area of focus in **(B).** Arrows indicate the gliotic scar around the developing cavity (DC), where IgG and IgM antibodies accumulate, as shown in (B). (B) Representative image of the injury epicenter (adjacent to the section shown in (A) stained for rat IgG (red), IgM (green) and counterstained with 4′,6-diamidino-2-phenylindole (DAPI). Red arrows show presence of IgM and IgG in the glial scar. White arrowheads show presence of IgG (red and yellow signal) and IgM (green and yellow signal) in the posterior white matter, and white arrows indicate presence of IgG in the anterior white matter. **(C-D)** Representative picture of spinal cord sections from a rat with SCI (C) and a sham control (D) at 2 weeks post-injury, stained for rat IgG immunoglobulins, glial fibrillary acidic protein (GFAP), and DAPI. IgG antibodies co-localized with astrocytes (white arrows) surrounding the DC. No co-labeling was detected in the spinal cord section of the sham rat (D). White inset in panel (C) indicates the area represented in images **(E)** and **(F)**. Scale bar: 100 μm. (E-F) Sections at the injury epicenter stained for IgG, IgM, DAPI, and GFAP (E) or chondroitin sulfate proteoglycans (CSPG; F). Panel (E) shows co-localization of endogenous IgG and IgM immunoglobulins with astrocytes (white signal) acquired by epifluorescence (i) and confocal (ii) microscope. Panel (F) shows co-localization of immunoglobulins with CSPG (white signal) as imaged with an epifluorescence (i) and a confocal (ii) microscope. Scale bar 20 μm (i) and 10 μm (ii). Color image is available online at www.liebertpub.com/neu

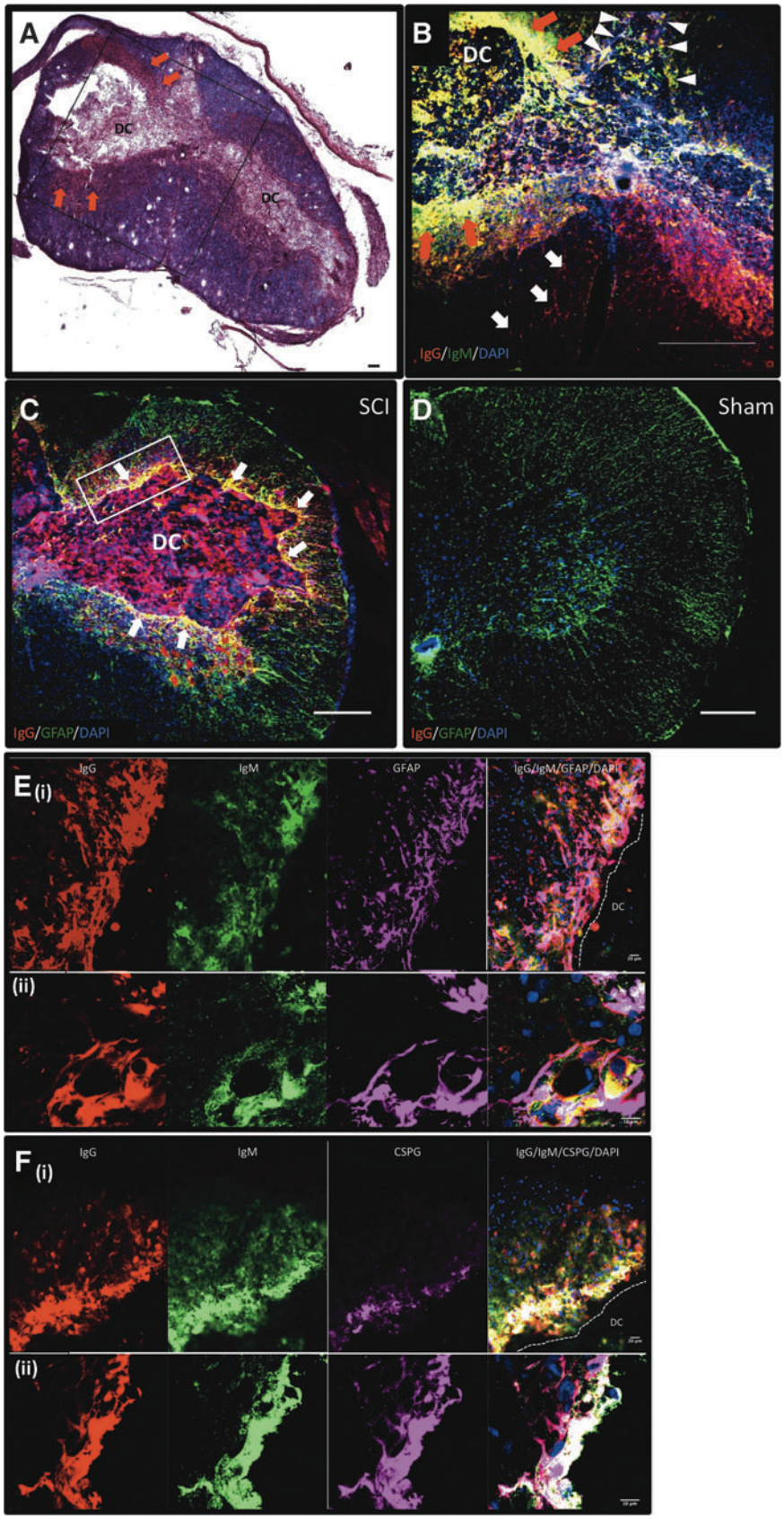
A
DC
DC
B
DC
IgG/IgM/DAPI
C
SCI
DC
IgG/GFAP/DAPI
D
Sham
IgG/GFAP/DAPI
E (i)
IgG
IgM
GFAP
IgG/IgM/GFAP/DAPI
DC
(ii)
F (i)
IgG
IgM
CSPG
IgG/IgM/CSPG/DAPI
DC
(ii)

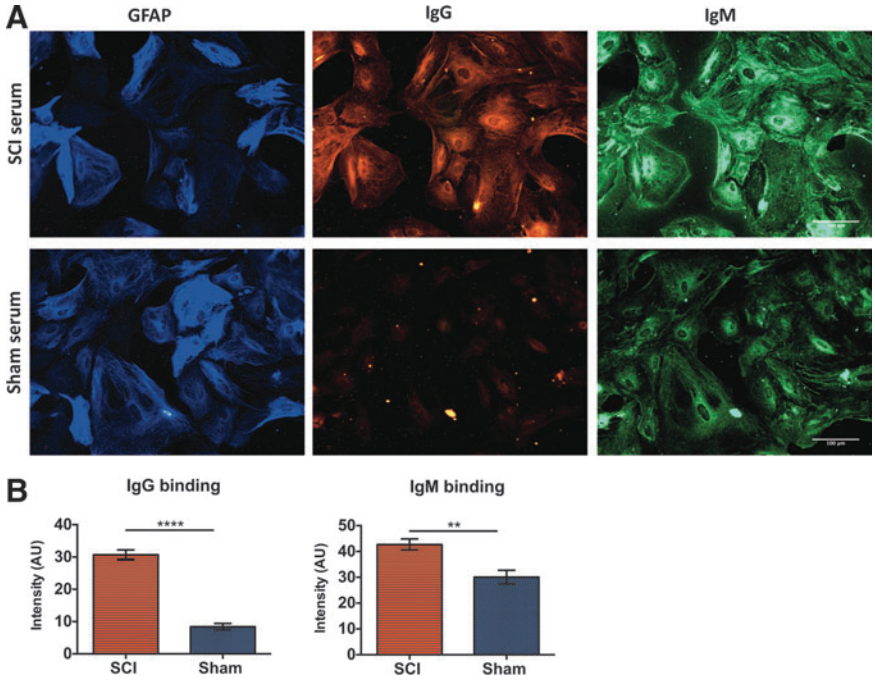

FIG. 4. Binding of serum immunoglobulins to astrocytes *in vitro.* **(A)** Representative image acquired with an epifluorescence microscope at 20× magnification, showing binding of serum IgG and IgM immunoglobulins to paraformaldehyde-fixed astrocytes. Scale bar: 100 μm. **(B)** Quantification of fluorescence intensity with ImageJ. Serum from rats with cervical spinal cord injury (cSCI) exhibited significantly higher binding to astrocytes, compared with shams. $^{**}p < 0.001$, $^{****}p < 0.00001$, $n = 5$/group, mean ± standard error of the mean. Color image is available online at www.liebertpub.com/neu

Discussion

This study characterizes the antibody response following cSCI in a rat model of compressive injury. We found increased antibody levels relative to sham animals in the injured spinal cord during the subacute phase of cSCI (2 weeks post-injury). We also identified the astroglial scar at the injury epicenter as one of the potential targets of antibodies following cSCI and showed that rats with cSCI harbored increased levels of serum IgG and IgM immunoglobulins against cultured astrocytes, compared with shams. Neurons of the ventral horn also were targeted by IgG immunoglobulins. Peripherally, at 2 weeks post-injury, increased ASC counts were observed in the spleen of rats with cSCI, compared with sham rats. Lastly, *in vitro* activation of splenocytes against homogenate of the injured spinal cord resulted in increased T-cell proliferation and IgG secretion. The above outcomes were similar between groups at 10 and

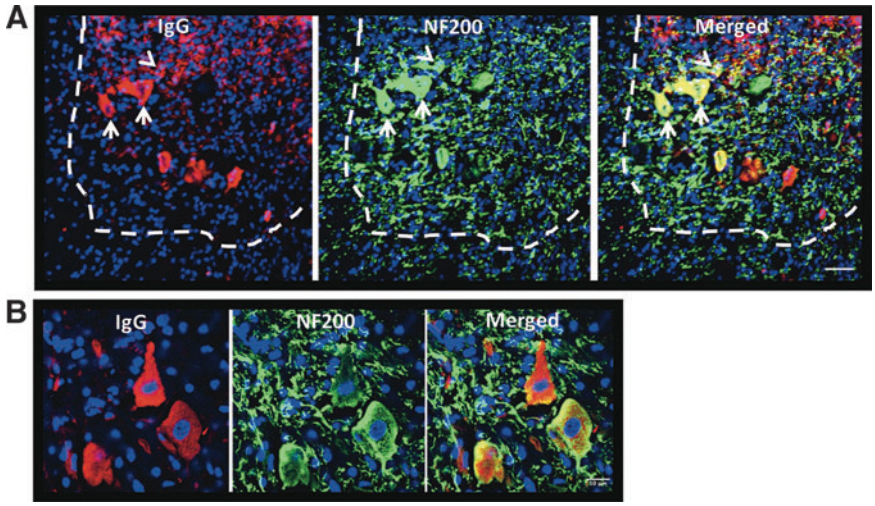

FIG. 5. Binding of IgG immunoglobulins to ventral horn neurons. **(A)** Immunostaining for rat IgG and NF200 at 2 weeks post–cervical spinal cord injury (cSCI). The ventral horn is located within the area indicated by the dashed line. IgG co-localized with NF200 in the gray but not in the white matter at the injury epicenter. In the gray matter, neuronal cell bodies of large (arrows) and smaller (arrowheads) neurons stained positive for IgG. Scale bar: 50 μm. **(B)** Confocal image of IgG+ neurons in the ventral horn. Scale bar: 10 μm. Color image is available online at www.liebertpub.com/neu

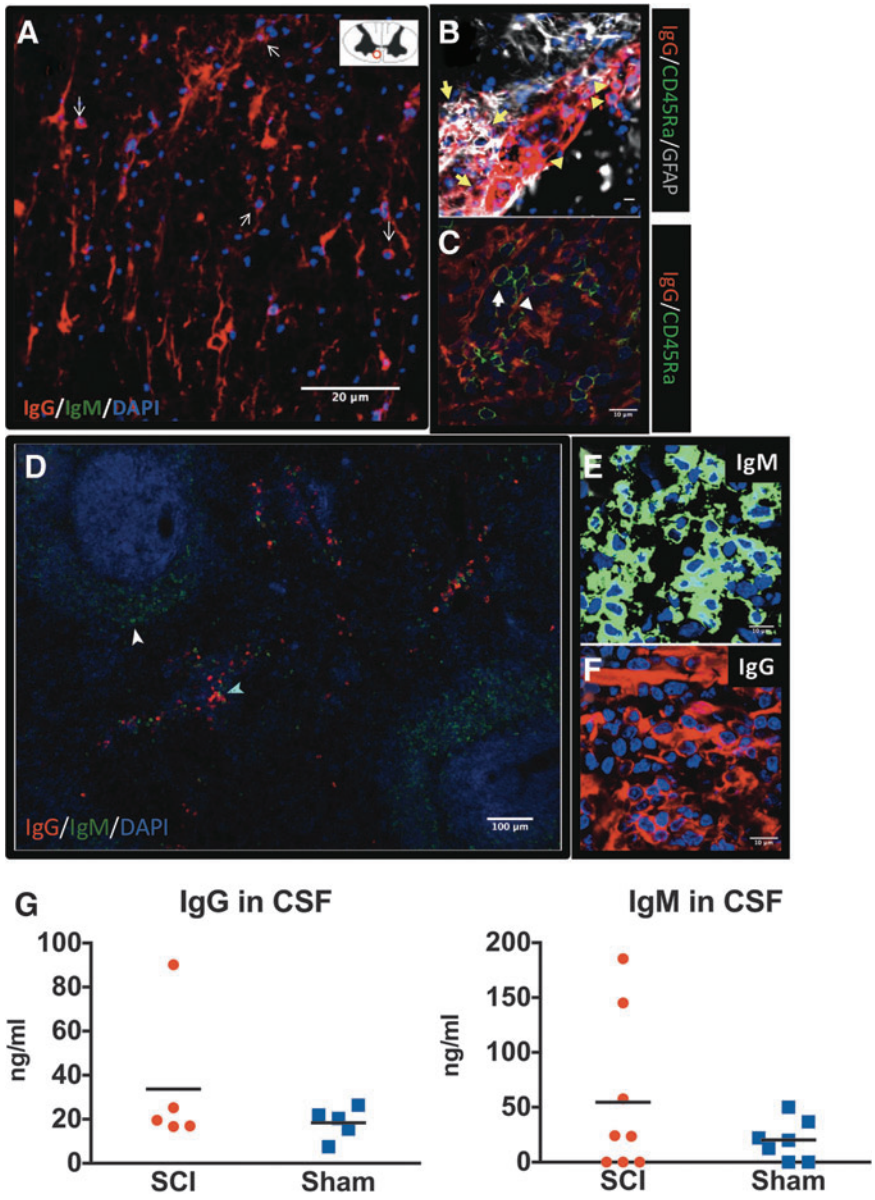

FIG. 6. Synthesis of immunoglobulin G (IgG) in the injured spinal cord at 2 weeks after cervical spinal cord injury (cSCI). **(A)** IgG+ antibody-secreting cells (ASCs) were detected in the lesioned spinal cord at 2 weeks post-SCI. Spinal cord sections were stained for rat IgG, IgM, and 4′,6-diamidino-2-phenylindole (DAPI) to assess presence of ASCs. IgG+ ASCs (arrows) were detected in the anterior white matter of the spinal cord, as shown in the schematic on the right corner of panel (A). IgM+ ASCs were not detected in the lesioned spinal cord. Scale bar: 20 μm. **(B)** Confocal microscope image taken close to the developing cavity distinguishing IgG+ ASCs (arrowhead) from IgG+ astrocytes (arrow) and lack of CD45RA expression in the IgG+ ASCs. **(C)** Rat spleen stained for CD45RA and IgG as a positive control for the detection of CD45RA+ cells. Of note, IgG+ ASCs (arrowhead) are negative for CD45RA staining (arrow). Scale bar (B, C): 10 μm. **(D)** Rat spleen stained for IgG and IgM immunoglobulins as a positive control for the detection of rat IgG+ (cyan arrowhead) and IgM+ (white arrowhead) ASCs. Scale bar: 100 μm. **(E-F)** High-power confocal image of splenic IgM+ and IgG+ ASCs. Scale bar: 10 μm. **(G)** Quantification of IgG and IgM immunoglobulins in cerebrospinal fluid (CSF) of SCI or sham rats at 2 weeks post-injury. Levels of immunoglobulins were not statistically different between the groups. Mann-Whitney test, $n = 5$-8/group; bars indicate mean. Color image is available online at www.liebertpub.com/neu

20 weeks post-injury, indicating that cSCI triggers a robust yet transient antibody immune response that does not persist in the chronic phase of injury, compared with sham injury.

The first novel finding of our study is the demonstration of presence of antibodies in the lesioned spinal cord following cSCI. However, spinal cord–directed antibodies are not part of the chronic pathology of cSCI, contrary to what is known for mid-thoracic injuries, where Ankeny and colleagues showed the presence of spinal cord autoantibodies in the chronic phase.[10] It is unknown whether the difference in the duration of autoantibody persistence in the lesioned spinal cord between our study and the study by Ankeny and colleagues is due to differences in injury level (cervical vs. mid-thoracic), the SCI model (compression vs. contusion), or the species used (rats vs. mice). Indeed, mice were shown to present with more prolonged cellular inflammation, compared with rats, following SCI,[22] which could

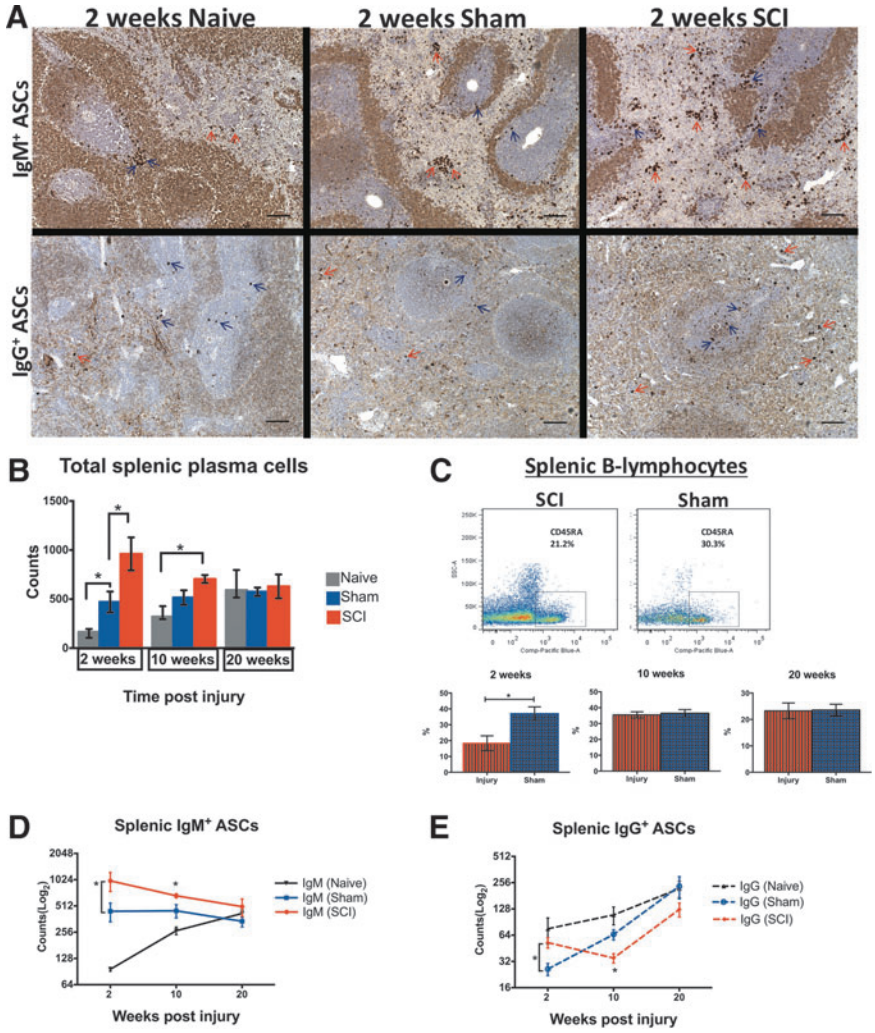

FIG. 7. Changes in splenic antibody-secreting cell (ASC) counts following cervical spinal cord injury (cSCI). **(A)** Representative brightfield microscopy images showing splenic immunoglobulin M (IgM)+ and IgG+ ASCs (or plasma cells) from age-matched naïve, sham, and SCI rats at 2 weeks post-injury. Red arrows indicate ASCs in the red pulp and blue arrows show ASCs in the white pulp of the spleen. Scale bar: 100 μm. **(B)** Total splenic ASC counts in naïve, sham, and SCI rats at 2, 10, and 20 weeks post-injury. At 2 weeks, the cSCI group had higher plasma cell counts than sham controls. Also, sham animals had higher counts of splenic ASCs than age-matched naïve rats. There was no significant difference in total plasma cell counts at subsequent time-points between animals with cSCI and sham injury or between naïve and sham animals, although ASC counts were higher in the cSCI group than in age-matched naïve controls at 10 weeks. $*p < 0.05$, one-way analysis of variance for each time-point with Bonferroni *post hoc* test, $n = 6$-8/group, mean ± standard error of the mean (SEM). **(C)** Changes in frequency of splenic B-cells at 2, 10, and 20 weeks post-injury. Top: Representative dot plot panels showing the gated population of B-lymphocytes out of viable CD45+ cells (leukocytes) in the spleen of a spinally injured and a sham rat at 2 weeks post-injury. Bottom: Changes in percent frequencies (%) of splenic B-cells at 2, 10, and 20 weeks post-injury. B-lymphocytes declined significantly at 2 weeks post-injury, compared with shams, but recovered to normal levels at subsequent time-points. $*p < 0.05$, Independent Student's *t*-test, $n = 6$/group, mean ± SEM. **(D-E)** Quantification of IgM+ and IgG+ ASCs in the spleen of naïve, sham and SCI rats at 2, 10, and 20 weeks post-injury. Asterisks indicate significant differences between SCI and sham groups only. (D) IgM+ ASC counts increased significantly at 2 and 10 weeks post-cSCI, compared with shams. At 20 weeks, there was no significant difference between groups. (E) IgG+ ASC counts increased at 2 weeks but declined significantly at 10 weeks post-cSCI, compared with shams. IgG+ ASC counts were similar between groups at 20 weeks. Color image is available online at www.liebertpub.com/neu

explain the chronicity in the development of autoantibodies in the study by Ankeny and colleagues. The effect of the level of injury on autoantibody responses also may explain the difference in findings between our study and that by Ankeny and colleagues. Ankeny and colleagues evaluated the development of autoantibodies after T9 injury. However, injuries at T9 leave humoral responses intact partly because the sympathetic innervation of the spleen is largely preserved.[13–15,23] Injuries at the cervical level, on the other hand, presumably disrupt normal sympathetic innervation of the spleen, potentially terminating the autoantibody response earlier.

The exact mechanisms that limit autoantibody responses to the subacute phase in cSCI are elusive. However, once known, we could leverage these mechanisms to restrict detrimental humoral responses in SCI cases (such as thoracic-level injuries) where autoantibodies persist in the chronic phase.[10] Further work is required to confirm that the level of SCI affects the magnitude of antibody autoimmune responses.

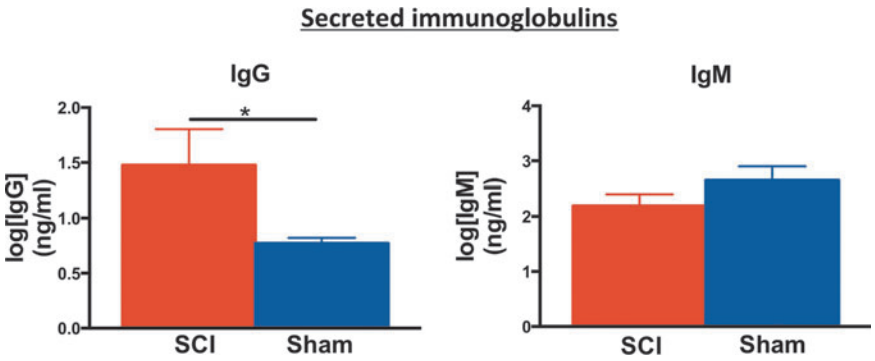

FIG. 8. Levels of immunoglobulin G (IgG) and IgM secreted by splenocytes *in vitro.* Higher levels of IgG immunoglobulins, but not IgM, were secreted by splenocytes from animals with cSCI when stimulated with injured spinal cord homogenate. Note that the concentration of immunoglobulins is transformed to log scale to allow for appropriate statistical analysis. Mann-Whitney test, $*p < 0.05$, $n = 4$/group, mean ± standard error of the mean. Color image is available online at www.liebertpub.com/neu

We identified neurons of the ventral horn and perilesional astrocytes as some of the cell types that are targeted by autoantibodies in the lesioned spinal cord. Previous studies have demonstrated localization of immunoglobulins to astrocytes[24] and neurons with motoneuron morphology[10] in animal models of thoracic injury. Development of autoantibodies against astrocytes and neurons is an observation of substantial clinical relevance; antibodies against astrocytes are the hallmark of neuromyelitis optica—an autoantibody-mediated demyelinating disease of the optic nerve and the spinal cord[25]—whereas antibodies against neurons (including motoneurons), have been associated with a number of autoimmune channelopathies in the CNS.[26] Deposition of IgG on neurons may result from their function as a ''sink'' for extravasated plasma proteins after changes in their membrane permeability due to injury,[27,28] or as a result of retrograde transport from outside the CNS through motoneurons of the spinal cord, whose axons project into the periphery.[29–33] Similarly, IgG binding to astrocytes may result from sequestration of immunoglobulins that are extravasated into the CNS due to the breakdown of the BSCB in order to maintain homeostasis after injury.[19]

To test the latter hypothesis, we measured binding of serum immunoglobulins from rats with sham or cSCI injury at 2 weeks to fixed astrocytes, which cannot engage in sequestration. Our discovery of higher binding of SCI-derived immunoglobulins, compared with controls, supports that deposition of antibodies in the injured spinal cord at 2 weeks is autoimmune in nature; this result does not exclude sequestration as an additional mechanism *in vivo. In vitro,* both IgG and IgM immunoglobulins bound to structures of the astrocytic cytoskeleton, such as GFAP. Interestingly, higher levels of GFAP protein have been detected in the blood of patients with neurotrauma,[34] and recent studies have shown that patients with traumatic brain injury have significantly higher levels of autoantibodies against GFAP than healthy controls.[35] Together, these findings may suggest the possibility that astrocytic GFAP enters the circulation after injury to reach the peripheral organs of the immune system (e.g., spleen) where it triggers an autoimmune response culminating in the generation of anti-GFAP autoantibodies.

Immunoglobulins of the spinal cord parenchyma may originate from circulation or may be synthesized *in situ* by resident ASCs. Identifying the source of these antibodies can help us design interventions that best target their pathogenic effects.[10] Similar to previous research in a thoracic SCI model,[10] we detected IgG+ ASCs in the lesioned spinal cord, demonstrating that some parenchymal IgG synthesis may take place in the subacute phase of cSCI. High affinity for neo-epitopes in the injured spinal cord in addition to a gradient of appropriate chemokines could facilitate the recruitment of ASCs at the injury epicenter.[36] These ASCs were distinct from IgG+ astrocytes and were negative for the B-cell marker CD45RA. In fact, we did not detect any CD5RA+ cells in the spinal cord of injured rats, a finding similar to results from studies in humans with SCI.[37] Moreover, because the integrity of the BSCB to large molecules is still compromised during the subacute phase,[38,39] it is possible that the majority of the IgG immunoglobulins in the spinal cord originate from the pool of circulating antibodies that extravasated in the spinal cord parenchyma. Lack of IgM+ ASCs in the spinal cord suggests that higher IgM immunoglobulins detected in the lesioned spinal cord at 2 weeks derive exclusively from the systemic pool of antibodies. Moreover, similar levels of total CSF immunoglobulins between sham and SCI rats exclude intrathecal synthesis as a potential source of antibodies within the lesioned spinal cord. Indeed, to the best of our knowledge, there is no compelling evidence to date to support that levels of immunoglobulins in CSF increase as a result of SCI. Previous studies have shown presence of immunoglobulins in mice or patients with SCI, but no data from sham or healthy controls were presented.[10,40,41]

Increased immunoglobulins within the lesioned cervical cord at 2 weeks post-cSCI were seen in parallel with increased counts of ASCs in the spleen, suggesting that the spleen may be one of the sources of autoantibodies targeting the spinal cord. Other sources, such as the bone marrow and the regional lymph nodes that receive antigenic drainage from the spinal cord,[42] also could contribute to the pool of autoantibodies against the spinal cord in the subacute phase.

An unexpected finding of our study is the observation of increased IgM+ ASCs in the spleen at 2 and 10 weeks following cSCI. Splenic IgM+ ASCs derive from non-switched B2 cells, marginal zone (MZ) B-cells, and B1-cells; the latter two cell types provide a rapid and polyreactive humoral response to blood-borne T--independent (TI) antigens.[43] Additionally we found IgG+ ASCs to be higher at 2 weeks but to decline at 10 weeks post-injury. Typically, IgG+ ASCs emerge as a result of high affinity TD immune responses. Thus, our results suggest that cSCI enhances TD and TI immune responses in the subacute phase. However, in the chronic phase, TD humoral responses decay, whereas TI responses persist.

The effect of higher IgM+ ASC counts on the progression of cSCI is unknown. It is possible that IgM+ ASCs increase in order to synthesize natural IgM immunoglobulins as a rapid mechanism to compensate for the massive cell death and overall disruption of homeostasis following SCI. Indeed, natural IgM immunoglobulins are low-affinity, polyreactive germline antibodies that maintain

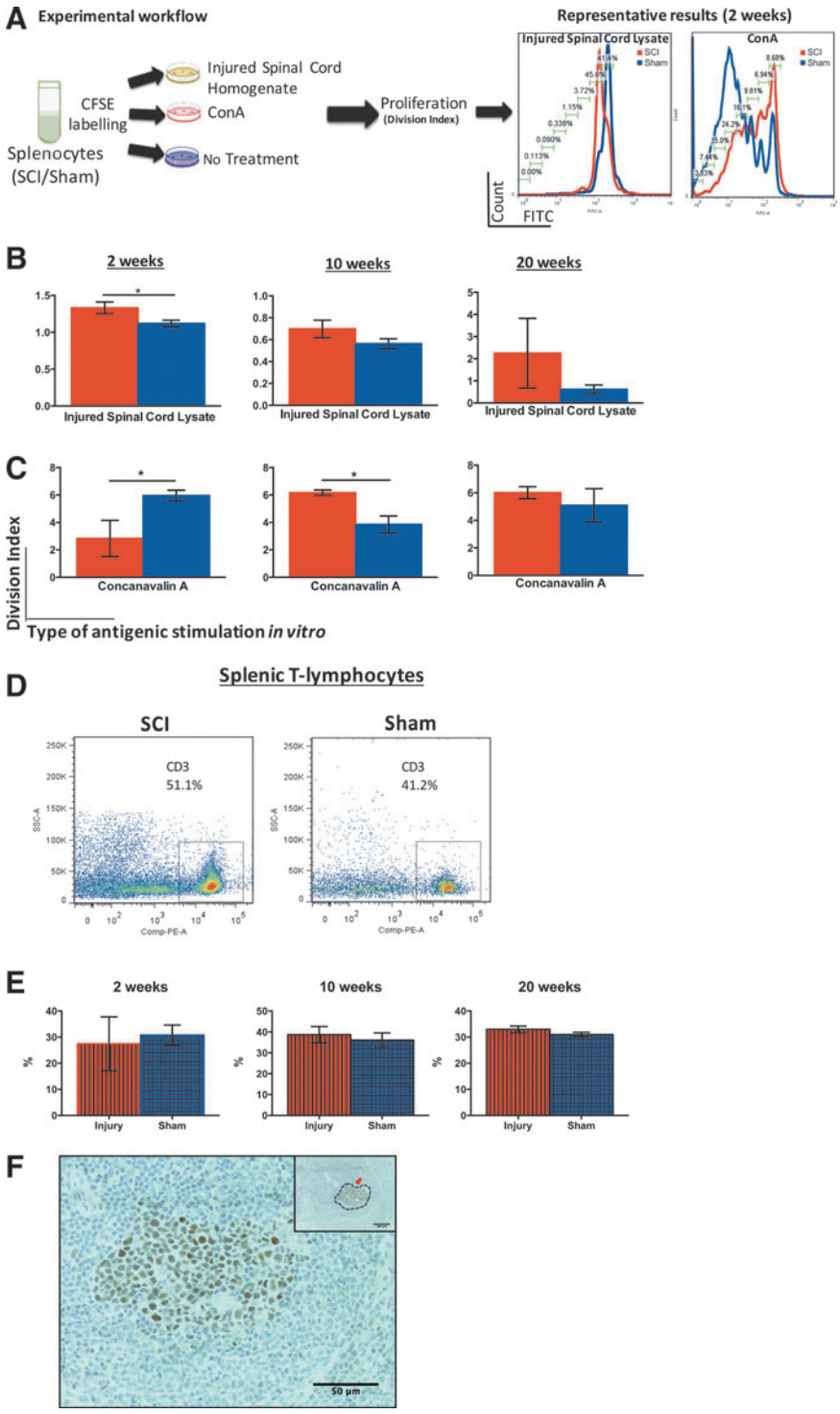

FIG. 9. Autoreactive T-dependent (TD) response *in vitro* following cervical spinal cord injury (cSCI). **(A)** Experimental workflow for the study of splenic T-cell proliferation *in vitro* and representative results indicating proliferation of T-cells when stimulated with injured spinal cord homogenate or Concanavalin A (ConA) at 2 weeks post-cSCI. Each peak of the histogram represents one cycle of cell division. The indicated percentage of cells in each cell cycle refers to the SCI group. **(B)** Proliferation (shown as division index) of splenic T-cells isolated from rats with cSCI or sham injury at 2, 10, and 20 weeks post-injury, after *in vitro* stimulation with homogenate from injured spinal cord at 2, 10, and 20 weeks post-injury, respectively. SCI-derived splenic T-cells proliferated more rapidly, compared with sham-derived splenocytes, at 2 weeks post-injury, but not at later time-points. **(C)** Proliferation of splenic T-cells isolated from rats with cSCI or sham injury at 2, 10, and 20 weeks post-injury after *in vitro* stimulation with ConA. At 2 weeks, SCI-derived T-cells showed less proliferation, compared with their sham counterparts. Contrary, at 10 weeks post-injury, SCI-derived splenic T-cells proliferated more than sham-derived T-cells. There was no significant difference at 20 weeks post-SCI. **(D)** Representative dot-plot image acquired with flow cytometry indicating the percent frequency (%) of splenic T-lymphocytes (CD3+) out of total viable leukocytes (CD45+) in SCI and sham rats at 2 weeks. **(E)** Changes in percent frequency (%) of splenic T-cells at 2, 10 and 20 weeks post-SCI. No significant alterations in T-cell frequency occur in the SCI group, compared with shams. Mann-Whitney test (B-C), Independent Student's *t*-test (E), $*p < 0.05$, $n = 4$/group (B-C), $n = 6$/group (D-E), mean ± standard error of the mean. **(F)** Development of germinal centers in the spleen of rats at 2 weeks post-cSCI. Representative image of a spleen section stained for Bcl-6 indicating a germinal center. The inset is a lower power image demonstrating the location of the germinal center within the white pulp of the spleen. Color image is available online at www.liebertpub.com/neu

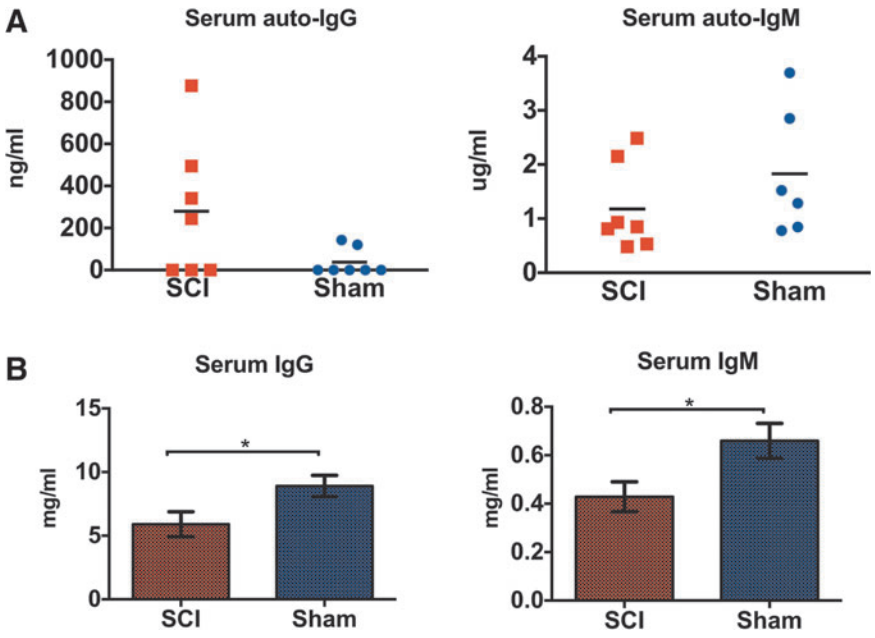

FIG. 10. Effects of cervical spinal cord injury (cSCI) in levels of autoreactive and total immunoglobulins in serum. **(A)** Quantification of autoreactive serum immunoglobulin G (IgG) and IgM against spinal cord lysate in rats with cSCI or sham injury at 2 weeks. There was no statistically significant difference between the groups. Mann-Whitney test, $n = 7$/group (IgG), Independent Student's *t*-test, $n = 6$-7/group (IgM), Bars indicate mean. **(B)** Quantification of total serum IgG and IgM immunoglobulins in SCI or sham rats at 2 weeks. IgG and IgM immunoglobulins declined significantly as a result of cSCI. Independent Student's *t*-test, $*p < 0.05$, $n = 6$-9/group, mean ± standard error of the mean. Color image is available online at www.liebertpub.com/neu

homeostasis by rapidly clearing up microbial pathogens and apoptotic cells.[44] In addition, they inhibit the emergence of autoreactive IgG responses, thereby conveying protection against detrimental humoral autoimmunity.[45–48] Splenic B1 cells[49] and a subset of bone marrow B1 cells[50,51] constitute the main sources of circulating natural IgM immunoglobulins. Therefore, it is possible that IgM+ ASCs in the spleen increase as a compensatory mechanism to resolve homeostasis after cSCI. Notably, this response may result in the development of remyelinating IgM clones.[52] Alternatively, increased IgM+ ASC counts in the spleen may support the emergence of IgM autoantibodies against components of the spinal cord, as is the case for a number of neuropathies where patients present with high titers of IgM antibodies against gangliosides.[53–55] Thus, more research is needed to dissect whether splenic IgM+ ASCs play a key role in the pathophysiology of SCI.

Despite the prevalence of IgM+ ASCs in the spleen, and the increased levels of IgM immunoglobulins in the spinal cord, we did not detect higher levels of secreted IgM antibodies in our *in vitro* stimulation assay. This inconsistency likely reflects a limitation of our experimental approach, which was not optimally designed to study IgM immune responses *in vitro.* In particular, we stimulated splenocytes with spinal cord homogenate, in which the composition of non-protein components (i.e., lipids and carbohydrates) is unknown. Thus, it is possible that the concentration of non-protein molecules (which drive IgM immunity) in the homogenate was too low to effectively stimulate an IgM response *in vitro.*[44] Perhaps different antigen extraction methods or the use of purified antigens is needed to stimulate IgM secretion in this assay. Therefore, although relevant in studying IgG responses, this stimulation paradigm does not accurately reflect the splenic IgM responses that occur *in vivo.*

Higher levels of IgG antibodies in the lesioned spinal cord during the subacute injury phase were seen in parallel with enhanced TD splenic responses, as shown *in vitro* by pronounced splenic T-cell proliferation and the increased secretion of IgG immunoglobulins in response to stimulation from injured spinal cord homogenate, and *in vivo* by the development of germinal centers in the spleen of rats with cSCI. These results suggest that T-cells are involved in the antibody response against the spinal cord early after cSCI. Popovich and colleagues found no significant proliferation of splenic T-lymphocytes when stimulated with MBP, suggesting that T-cells do not elicit a significant autoreactive response against MBP after thoracic SCI in rats.[56] It is, however, difficult to truly compare the differing results between our study and that of Popovich and colleagues because our stimulation protocols are substantially different. Here we chose to stimulate with total homogenate from the injured spinal cord rather than MBP because the exact antigens that could stimulate the spleen after cSCI are unknown. Nevertheless, studies in thoracic SCI models suggest that autoreactive T-lymphocytes are key to the pathology and recovery of SCI.[57,58] In our study, we extend the observations made in thoracic models by demonstrating that autoreactive TD immune responses are induced in the subacute phase of cSCI.

Interestingly, at 2 weeks, rats with cSCI had a compromised response to polyclonal stimulation by ConA i*n vitro,* harbored less splenic B-cells, and had significantly reduced levels of serum IgG and IgM immunoglobulins; together, these findings suggest a state of general immunosuppression following cSCI. Particularly, decreased total levels of immunoglobulins in serum despite the elevated ASC counts in the spleen suggest that antibody synthesis in the bone marrow may be substantially disrupted in rats with cSCI. Indeed, the mature immune cells in the bone marrow of patients with SCI exhibit depressed function and the progenitor cells have impaired proliferation capacity.[59] Together, these data are consistent with the evidence for the development of immunosuppression

after SCI.[60–64] Interestingly, at the peak of pronounced immune compromise (2 weeks after injury), we also observed enhanced autoreactive splenic activation. Indeed, this ''paradox'' of co-existing immune suppression and autoimmunity is a common concept in systemic autoimmune diseases,[65] and is now recognized as part of SCI pathology.[66] Intravenous immunoglobulin G administration could address this duality of the immune response after SCI,[67,68] given that it is successfully used both as an immune replacement for immunosuppressed individuals, and as an immunosuppressant for autoimmune diseases.[69]

Despite the increased antibody levels in the lesioned spinal cord and the splenic autoreactive response *in vitro* during the subacute phase of cSCI, we did not find increased levels of serum autoantibodies against spinal cord proteins by ELISA. There can be at least three non-mutually exclusive explanations for this result: a) lowered levels of total serum antibodies in injured rats, compared with shams, mask the detection of any potential increase in autoantibody titers as a result of cSCI; b) the antigens that are targeted by autoantibodies within the spinal cord are too diluted or absent in the protein extract preparation used for ELISA; thereby, a replication of the autoreactivity in the spinal cord tissue may not be favorable *in vitro*; and c) the serum is largely devoid of autoantibodies against the spinal cord, as they preferentially extravasate and deposit in the lesioned spinal cord. For these reasons, serum antibody autoreactivity against whole spinal cord lysate may be of little clinico-pathological value. Instead, investigating reactivity against specific components of the spinal cord may be more useful. As our work and other research suggests, astrocytic proteins might be a target for the autoantibody response.[24,35]

Conclusion

In conclusion, our study characterizes the antibody response following cSCI and provides evidence for the development of antibodies against the spinal cord in the subacute phase of experimental cSCI. This finding adds to our understanding of the immune-mediated pathology of SCI at the cervical level, which remains largely unexplored despite its prevalence in clinical SCI.[70] The significance of this discovery for outcomes after cSCI remains to be investigated. However, the relatively limited duration of the autoantibody response in the cervical spinal cord, compared with thoracic injury, suggests that potential interventions aimed at the autoantibody response should be tailored to the level of SCI.

We anticipate that the current study will be a foundation for future research to characterize the role and mechanisms of action of autoantibodies after cSCI, with the ultimate objective of developing effective immune-based treatments for human SCI.

Acknowledgments

We are thankful to Stem Cell Network for supporitng AU with a bursary to learn flow cytometry at the University of British Columbia Flow Cytometry Facility. We also thank Drs. Joan Wither and Tania Watts for their constructive feedback throughout the course of this study, Drs. Pia Vidal and Nicole Forgione for their feedback during the preparation of this manuscript, and Dr. Madeleine O' Higgins for copyediting this manuscript. MGF is supported by the Halbert Chair in Neural Repair and Regeneration and the DeZwirek Foundation.

Author Disclosure Statement

No competing financial interests exist.

References

1. Dvorak, M. F. Noonan, V.K., Fallah, N., Fisher, C.G., Rivers, C.S., Ahn, H., Tsai, E.C., Linassi, A.G., Christie, S.D., Attabib, N., Hurlbert, R.J., Fourney, D.R., Johnson, M.G., Fehlings, M.G., Drew, B., Bailey, C.S., Paquet, J., Parent, S., Townson, A., Ho, C., Craven, B.C., Gagnon, D., Tsui, D., Fox, R., Mac-Thiong, J.M., and Kwon, B.K. (2014). Minimizing errors in acute traumatic spinal cord injury trials by acknowledging the heterogeneity of spinal cord anatomy and injury severity: an observational Canadian cohort analysis. J. Neurotrauma 31, 1540–1547.
2. The National Spinal Cord Injury Statistical Center (2015). Spinal Cord Injury: facts and figures at a glance. Available at: www.nscisc.uab.edu. Accessed December 5. 2015.
3. Sekhon, L. H. and Fehlings, M. G. (2001). Epidemiology, demographics, and pathophysiology of acute spinal cord injury. Spine 26, S2–S12.
4. Fehlings, M., Singh, A., Tetreault, L., Kalsi-Ryan, S., and Nouri, A. (2014). Global prevalence and incidence of traumatic spinal cord injury. Clin. Epidemiol. 6, 309–331.
5. Donnelly, D. J. and Popovich, P. G. (2008). Inflammation and its role in neuroprotection, axonal regeneration and functional recovery after spinal cord injury. Exp. Neurol. 209, 378–388.
6. Kwon, B. K., Hillyer, J., and Tetzlaff, W. (2010). Translational research in spinal cord injury: a survey of opinion from the SCI community. J. Neurotrauma 27, 21–33.
7. Davies, A. L., Hayes, K.C., and Dekaban, G.A. (2007). Clinical correlates of elevated serum concentrations of cytokines and autoantibodies in patients with spinal cord injury. Arch. Phys. Med. Rehabil. 88, 1384–1393.
8. Hayes, K.C. Hull, T.C., Delaney, G.A., Potter, P.J., Sequeira, K.A., Campbell, K., and Popovich, P.G. (2002). Elevated serum titers of proinflammatory cytokines and CNS autoantibodies in patients with chronic spinal cord injury. J. Neurotrauma 19, 753–761.
9. Saltzman, J.W. Battaglino, R.A., Salles, L., Jha, P., Sudhakar, S., Garshick, E., Stott, H.L., Zafonte, R., and Morse, L.R. (2013). B-cell maturation antigen, a proliferation-inducing ligand, and B-cell activating factor are candidate mediators of spinal cord injury-induced autoimmunity. J. Neurotrauma 30, 434–440.
10. Ankeny, D.P., Guan, Z., and Popovich, P.G. (2009). B cells produce pathogenic antibodies and impair recovery after spinal cord injury in mice. J. Clin. Invest. 119, 2990–2999.
11. Wu, B. Matic, D., Djogo, N., Szpotowicz, E., Schachner, M., and Jakovcevski, I. (2012). Improved regeneration after spinal cord injury in mice lacking functional T- and B-lymphocytes. Exp. Neurol. 237, 274–285.
12. Ankeny, D.P., Lucin, K.M., Sanders, V.M., McGaughy, V.M., and Popovich, P.G. (2006). Spinal cord injury triggers systemic autoimmunity: evidence for chronic B lymphocyte activation and lupus-like autoantibody synthesis. J. Neurochem. 99, 1073–1087.
13. Ibarra, A., Jiménez, A., Cortes, C., and Correa, D. (2007). Influence of the intensity, level and phase of spinal cord injury on the proliferation of T cells and T-cell-dependent antibody reactions in rats. Spinal Cord 45, 380–386.
14. Lucin, K.M., Sanders, V.M., Jones, T.B., Malarkey, W.B., and Popovich, P.G. (2007). Impaired antibody synthesis after spinal cord injury is level-dependent and is due to sympathetic nervous system dysregulation. Exp. Neurol. 207, 75–84.
15. Lucin, K.M., Sanders, V.M., and Popovich, P.G. (2009). Stress hormones collaborate to induce lymphocyte apoptosis after high level spinal cord injury. J. Neurochem. 110, 1409–1421.
16. Fehlings, M.G. and Tator, C.H. (1995). The relationships among the severity of spinal cord injury, residual neurological function, axon counts, and counts of retrogradely labeled neurons after experimental spinal cord injury. Exp. Neurol. 132, 220–228.
17. Anderson, D.K. Beattie, M., Blesch, A., Bresnahan, J., Bunge, M., Dietrich, D., Dietz, V., Dobkin, B., Fawcett, J., Fehlings, M., Fischer, I., Grossman, R., Guest, J., Hagg, T., Hall, E.D., Houle, J., Kleitman, N., McDonald, J., Murray, M., Privat, A., Reier, P., Steeves, J., Steward, O., Tetzlaff, W., Tuszynski, M.H., Waxman, S.G., Whittemore, S., Wolpaw, J., Young, W., and Zheng, B. (2005). Recommended guidelines for studies of human subjects with spinal cord injury. Spinal Cord 43, 453–458.
18. Zhang, J. (2000). Protein-length distributions for the three domains of life. Trends Genet. 16, 107–109.

19. Bernstein, J.J., Willingham, L.A., and Goldberg, W.J. (1993). Sequestering of immunoglobulins by astrocytes after cortical lesion and homografting of fetal cortex. Int. J. Dev. Neurosci. 11, 117–124.
20. Benner, R., Rijnbeek, A.M., Bernabé, R. R., Martinez-Alonso, C., and Coutinho, A. (1981). Frequencies of background immunoglobulin-secreting cells in mice as a function of organ, age, and immune status. Immunobiology 158, 225–238.
21. Mothe, A.J. Bozkurt, G., Catapano, J., Zabojova, J., Wang, X., Keating, A., and Tator, C.H. (2011). Intrathecal transplantation of stem cells by lumbar puncture for thoracic spinal cord injury in the rat. Spinal Cord 49, 967–973.
22. Sroga, J.M., Jones, T.B., Kigerl, K.A., McGaughy, V.M., and Popovich, P.G. (2003). Rats and mice exhibit distinct inflammatory reactions after spinal cord injury. J. Comp. Neurol. 462, 223–240.
23. Oropallo, M.A., Held, K.S., Goenka, R., Ahmad, S.A., O'Neill, P.J., Steward, O., Lane, T.E., and Cancro, M.P. (2012). Chronic spinal cord injury impairs primary antibody responses but spares existing humoral immunity in mice. J. Immunol. 188, 5257–5266.
24. Bernstein, J.J. and Goldberg, W.J. (1987). Injury-related spinal cord astrocytes are immunoglobulin-positive (IgM and/or IgG) at different time periods in the regenerative process. Brain Res. 426, 112–118.
25. Lennon, V.A., Kryzer, T.J., Pittock, S.J., Verkman, A.S., and Hinson, S.R. (2005). IgG marker of optic-spinal multiple sclerosis binds to the aquaporin-4 water channel. J. Exp. Med. 202, 473–477.
26. Vincent, A., Lang, B., and Kleopa, K.A. (2006). Autoimmune channelopathies and related neurological eisorders. Neuron 52, 123–138.
27. Brightman, M.W., Klatzo, I., Olsson, Y., and Reese, T.S. (1970). The blood-brain barrier to proteins under normal and pathological conditions. J. Neurol. Sci. 10, 215–239.
28. Povlishock, J.T., Becker, D.P., Miller, J.D., Jenkins, L.W., and Dietrich, W.D. (1979). The morphopathologic substrates of concussion? Acta Neuropathol. (Berl.) 47, 1–11.
29. Aihara, N., Tanno, H., Hall, J.J., Pitts, L.H., and Noble, L.J. (1994). Immunocytochemical localization of immunoglobulins in the rat brain: relationship to the blood-brain barrier. J. Comp. Neurol. 342, 481–496.
30. Fabian, R.H. (1986). Intraneuronal IgG in the central nervous system. J. Neurol. Sci. 73, 257–267.
31. Fabian, R.H. (1990). Uptake of antineuronal IgM by CNS neurons: comparison with antineuronal IgG. Neurology 40, 419–422.
32. Yamamoto, T., Iwasaki, Y., Konno, H., Iizuka, H., and Zhao, J.X. (1987). Retrograde transport and differential accumulation of serum proteins in motor neurons: implications for motor neuron diseases. Neurology 37, 843–846.
33. Yoshimi, K., Woo, M., Son, Y., Baudry, M., and Thompson, R.F. (2002). IgG-immunostaining in the intact rabbit brain: variable but significant staining of hippocampal and cerebellar neurons with anti-IgG. Brain Res. 956, 53–66.
34. Petzold, A. (2015). Glial fibrillary acidic protein is a body fluid biomarker for glial pathology in human disease. Brain Res. 1600, 17–31.
35. Wang, K.K.W., Yang, Z., Yue, J.K., Zhang, Z., Winkler, E.A., Puccio, A.M., Diaz-Arrastia, R., Lingsma, H.F., Yuh, E.L., Mukherjee, P., Valadka, A.B., Gordon, W.A., Okonkwo, D.O., Manley, G.T., Cooper, S.R., Dams-O'Connor, K., Hricik, A.J., Inoue, T., Maas, A.I., Menon, D.K., Schnyer, D.M., Sinha, T.K., and Vassar, M.J. (2016). Plasma anti-glial fibrillary acidic protein autoantibody levels during the acute and chronic phases of traumatic brain injury: a transforming research and clinical knowledge in traumatic brain injury pilot study. J. Neurotrauma 33, 1270–1277.
36. Marques, C.P. Kapil, P., Hinton, D.R., Hindinger, C., Nutt, S.L, Ransohoff, R.M., Phares, T.W., Stohlman, S.A., and Bergmann, C.C. (2011). CXCR3-dependent plasma blast migration to the central nervous system during viral encephalomyelitis. J. Virol. 85, 6136–6147.
37. Fleming, J.C. Norenberg, M.D., Ramsay, D.A., Dekaban, G.A., Marcillo, A.E., Saenz, A.D., Pasquale-Styles, M., Dietrich, W.D., and Weaver, L.C. (2006). The cellular inflammatory response in human spinal cords after injury. Brain J. Neurol. 129, 3249–3269.
38. Figley, S.A., Khosravi, R., Legasto, J.M., Tseng, Y.F., and Fehlings, M.G. (2014). Characterization of vascular disruption and blood–spinal cord barrier permeability following traumatic spinal cord injury. J. Neurotrauma 31, 541–552.
39. Noble, L.J. and Wrathall, J.R. (1989). Distribution and time course of protein extravasation in the rat spinal cord after contusive injury. Brain Res. 482, 57–66.
40. Sengupta, M.B. Basu, M., Iswarari, S., Mukhopadhyay, K.K., Sardar, K.P., Acharyya, B., Mohanty, P.K., and Mukhopadhyay, D. (2014). CSF proteomics of secondary phase spinal cord injury in human subjects: perturbed molecular pathways post injury. PLOS ONE 9, e110885.
41. Carnini, A., Casha, S., Yong, V.W., Hurlbert, R.J., and Braun, J.E. (2010). Reduction of PrPC in human cerebrospinal fluid after spinal cord injury. Prion 4, 80–86.
42. Ransohoff, R.M. and Engelhardt, B. (2012). The anatomical and cellular basis of immune surveillance in the central nervous system. Nat. Rev. Immunol. 12, 623–635.
43. Martin, F., Oliver, A.M., and Kearney, J.F. (2001). Marginal zone and B1 B cells unite in the early response against T-independent blood-borne particulate antigens. Immunity 14, 617–629.
44. Ehrenstein, M.R. and Notley, C.A. (2010). The importance of natural IgM: scavenger, protector and regulator. Nat. Rev. Immunol. 10, 778–786.
45. Adib, M., Ragimbeau, J., Avrameas, S., and Ternynck, T. (1990). IgG autoantibody activity in normal mouse serum is controlled by IgM. J. Immunol. 145, 3807–3813.
46. Boes, M. (2000). Role of natural and immune IgM antibodies in immune responses. Mol. Immunol. 37, 1141–1149.
47. Boes, M. Schmidt, T., Linkemann, K., Beaudette, B.C., Marshak-Rothstein, A., and Chen, J. (2000). Accelerated development of IgG autoantibodies and autoimmune disease in the absence of secreted IgM. Proc. Natl. Acad. Sci. U. S. A. 97, 1184–1189.
48. Ehrenstein, M.R., Cook, H.T., and Neuberger, M.S. (2000). Deficiency in serum immunoglobulin (Ig)M predisposes to development of IgG autoantibodies. J. Exp. Med. 191, 1253–1258.
49. Holodick, N.E., Tumang, J.R., and Rothstein, T.L. (2010). Immunoglobulin secretion by B1 cells: differential intensity and IRF4-dependence of spontaneous IgM secretion by peritoneal and splenic B1 cells. Eur. J. Immunol. 40, 3007–3016.
50. Baumgarth, N., Waffarn, E.E., and Nguyen, T.T.T. (2015). Natural and induced B-1 cell immunity to infections raises questions of nature versus nurture. Ann. N. Y. Acad. Sci. 1362, 188–199.
51. Reynolds, A.E., Kuraoka, M., and Kelsoe, G. (2015). Natural IgM is produced by CD5− plasma cells that occupy a distinct survival niche in bone marrow. J. Immunol. 194, 231–242.
52. Watzlawik, J.O., Wootla, B., Painter, M.M., Warrington, A.E., and Rodriguez, M. (2013). Cellular targets and mechanistic strategies of remyelination-promoting IgMs as part of the naturally occurring autoantibody repertoire. Expert Rev. Neurother. 13, 1017–1029.
53. Niebroj-Dobosz, I., Janik, P., and Kwieciński, H. (2004). Serum IgM anti-GM1 ganglioside antibodies in lower motor neuron syndromes. Eur. J. Neurol. 11, 13–16.
54. Mori, A., Ueno, Y., Kuroki, T., Hoshino, Y., Shimura, H., Sekiguchi, Y., Noguchi, M., Hamada, Y., Kusunoki, S., Hattori, N., and Urabe, T. (2014). Motor-dominant polyneuropathy due to IgM monoclonal antibody against disialosyl gangliosides in a patient with mantle cell lymphoma. J. Neurol. Sci. 337, 215–218.
55. Brindel, I. Preud'homme, J.L., Vallat, J.M., Vincent, D., Vasquez, J.L., and Jauberteau, M.O. (1994). Monoclonal IgM reactive with several gangliosides in a chronic relapsing polyneuropathy. Neurosci. Lett. 181, 103–106.
56. Popovich, P.G., Stuckman, S., Gienapp, I.E., and Whitacre, C.C. (2001). Alterations in immune cell phenotype and function after experimental spinal cord injury. J. Neurotrauma 18, 957–966.
57. Hauben, E., Nevo, U., Yoles, E., Moalem, G., Agranov, E., Mor, F., Akselrod, S., Neeman, M., Cohen, I.R., and Schwartz, M. (2000). Autoimmune T cells as potential neuroprotective therapy for spinal cord injury. Lancet Lond. Engl. 355, 286–287.
58. Jones, T.B., Basso, D.M., Sodhi, A., Pan, J.Z., Hart, R.P., MacCallum, R.C., Lee, S., Whitacre, C.C., and Popovich, P.G. (2002). Pathological CNS autoimmune disease triggered by traumatic spinal cord injury: implications for autoimmune vaccine therapy. J. Neurosci. 22, 2690–2700.
59. Iversen, P.O., Hjeltnes, N., Holm, B., Flatebo, T., Strom-Gundersen, I., Ronning, W., Stanghelle, J., and Benestad, H.B. (2000). Depressed immunity and impaired proliferation of hematopoietic progenitor cells in patients with complete spinal cord injury. Blood 96, 2081–2083.
60. Failli, V., Kopp, M.A., Gericke, C., Martus, P., Klingbeil, S., Brommer, B., Laginha, I., Chen, Y., DeVivo, M.J., Dirnagl, U., and Schwab, J.M. (2012). Functional neurological recovery after spinal

cord injury is impaired in patients with infections. Brain J. Neurol. 135, 3238–3250.
61. Kopp, M.A., Druschel, C., Meisel, C., Liebscher, T., Prilipp, E., Watzlawick, R., Cinelli, P., Niedeggen, A., Schaser, K.D., Wanner, G.A., Curt, A., Lindemann, G., Nugaeva, N., Fehlings, M.G., Vajkoczy, P., Cabraja, M., Dengler, J., Ertel, W., Ekkernkamp, A., Martus, P., Volk, H.D., Unterwalder, N., Kölsch, U., Brommer, B., Hellmann, R.C., Saidy, R.R., Laginha, I., Prüss, H., Failli, V., Dirnagl, U., and Schwab, J.M. (2013). The SCIentinel study—prospective multicenter study to define the spinal cord injury-induced immune depression syndrome (SCI-IDS)—study protocol and interim feasibility data. BMC Neurol. 13, 168.
62. Riegger, T., Conrad, S., Liu, K., Schluesener, H.J., Adibzahdeh, M., and Schwab, J.M. (2007). Spinal cord injury-induced immune depression syndrome (SCI-IDS). Eur. J. Neurosci. 25, 1743–1747.
63. Riegger, T., Conrad, S., Schluesener, H.J., Kaps, H.P., Badke, A., Baron, C., Gerstein, J., Dietz, K., Abdizahdeh, M., and Schwab, J.M. (2009). Immune depression syndrome following human spinal cord injury (SCI): a pilot study. Neuroscience 158, 1194–1199.
64. Zhang, Y., Guan, Z., Reader, B., Shawler, T., Mandrekar-Colucci, S., Huang, K., Weil, Z., Bratasz, A., Wells, J., Powell, N.D., Sheridan, J.F., Whitacre, C.C., Rabchevsky, A.G., Nash, M.S., and Popovich, P.G. (2013). Autonomic dysreflexia causes chronic immune suppression after spinal cord injury. J. Neurosci. 33, 12970–12981.
65. Grammatikos, A.P. and Tsokos, G.C. (2012). Immunodeficiency and autoimmunity: lessons from systemic lupus erythematosus. Trends Mol. Med. 18, 101–108.
66. Schwab, J.M., Zhang, Y., Kopp, M.A., Brommer, B., and Popovich, P.G. (2014). The paradox of chronic neuroinflammation, systemic immune suppression, autoimmunity after traumatic chronic spinal cord injury. Exp. Neurol. 258, 121–129.
67. Nguyen, D.H., Cho, N., Satkunendrarajah, K., Austin, J.W., Wang, J., and Fehlings, M.G. (2012). Immunoglobulin G (IgG) attenuates neuroinflammation and improves neurobehavioral recovery after cervical spinal cord injury. J. Neuroinflammation 9, 224.
68. Tzekou, A. and Fehlings, M.G. (2014). Treatment of spinal cord injury with intravenous immunoglobulin G: preliminary evidence and future perspectives. J. Clin. Immunol. 34 Suppl 1, S132–138.
69. Jolles, S., Sewell, W., and Misbah, S. (2005). Clinical uses of intravenous immunoglobulin. Clin. Exp. Immunol. 142, 1–11.
70. Forgione, N., Karadimas, S.K., Foltz, W.D., Satkunendrarajah, K., Lip, A., and Fehlings, M.G. (2014). Bilateral contusion-compression model of incomplete traumatic cervical spinal cord injury. J. Neurotrauma 31, 1776–1788.

Address correspondence to:
Michael G. Fehlings, MD, PhD
Toronto Western Hospital
399 Bathurst Street, Suite 4W449
Toronto, Ontario, Canada M5T 2S8

E-mail: michael.fehlings@uhn.ca